The Reactions of Carbon Disulfide and Sulfur Dioxide with Small Carboxylate Anions

By
Zoe Anne Paula

A Thesis Submitted to
Saint Mary's University, Halifax, Nova Scotia
in Partial Fulfillment of the Requirements for
the Degree of Bachelor of Science
with Honours in Chemistry

April 2016, Halifax, Nova Scotia

Approved: Dr. Jason A.C. Clyburne
Supervisor
Department of Chemistry &
Environmental Science

Approved: Dr. Robert D. Singer
Chairperson
Department of Chemistry

Date: March 30, 2016

© Zoe Anne Paula, 2016

Abstract

In one form or another both acid gases and carboxylates have existed from prebiotic earth all the way to the present day. Here we have studied the reactions of carbon disulfide (CS_2) and sulfur dioxide (SO_2) with naked carboxylate anions ($RCOO^-$) to observe the types of interactions possible. The reaction of CS_2 with acetate (CH_3COO^-) in acetonitrile under an inert atmosphere proceeded via an exchange mechanism. This produced carbonyl sulfide gas (COS) and a thioacetate salt, which was characterized by X-ray crystallography. On the other hand, under the same conditions, the reaction of SO_2 with formate ($HCOO^-$) created a radical sulfur species. Overall, this led to the isolation of H_2 and CO_2 gases and to the formation of a number of possible $S_xO_y^{n-}$ species. Both reactions are thermodynamically stable enough to occur when salts of the anions, with large, non-coordinating cations, are exposed to the acid gases. The variety and biological importance of the products produced in these simple reactions show that their study may still hold many interesting and important new findings.

Acknowledgements

To start off, I have to thank my supervisor Dr. Jason Clyburne for giving me the opportunity to do my honors project at all. Working with him and the other members of the Clyburne group has been one of the best learning experiences I've had at Saint Mary's and has given me a new respect for chemistry. Jason never let me get discouraged and was always a good person to help figure out where to go next.

Without Dr. Kathy Robertson it is likely that this thesis wouldn't exist. Kathy has put in an enormous amount of work, keeping all of the Clyburne group on track this year with three different honors projects going on at the same time. Between handling the X-ray crystallography, helping to trouble shoot experiments and spending the time to edit this thesis so reading it is bearable, very little would get done around here without her.

I have to thank Juha Hurmalainen at the University of Jyväskylä in Finland and Michael Johnson at Dalhousie University for both helping out with the EPR experiments. While the conditions of the experiments did not lend themselves well to EPR, both of them were very patient with me, helping to find a way to make it work. And their findings ended up being essential in the final identification of the reaction products.

The wonderful staff here at Saint Mary's also deserves a huge thanks. Whether it was Patricia Granados, who spent a great deal of time helping me with separation techniques, or the technicians, helping me to track down all of the random things I needed, the entire process was smoothed over by them.

Last but not least I have to thank the other research students in the Clyburne group, both past and present. There isn't a single one of them who did not teach me something or help me somehow along the way. They have always made me feel welcome and this past year would not have been the same without them.

Table of Contents

List of Figures

List of Schemes

List of Tables

Table of Symbols and Abbreviations

eV	Electron volts
UV	Ultra violet
IR	Infrared
F^-	Fluoride anion
CN^-	Cyano anion
Å	Ångström
DBU	1,8-diazabicyclo[5.4.0]undec-7-ene
[BmPyrro][Ac]	1-butyl-1- methylpyrrolidinium acetate
DFT	Density Functional Theory
Cl^-	Chloride anion
I^-	Iodide anion
$[(CH_3)_4N^+]$	Tetramethyl ammonium cation
FSO_2^-	Fluorosulfite anion
SO_2I^-	Iodosulfite anion
$[BzTPP^+]$	Triphenyl benzyl phosphonium cation
°	Degree symbol
SO_2Cl^-	Chlorosulfite anion
SO_2CN^-	Cyanosulfite anion
$SO_2N_3^-$	Azidosulfite anion
[i-Pr$_2$Imes]	Imidazol-2-ylidene
au	Atomic Units
kJ/mol	Kilojules per mole
mM	Millimole
TBAA	Tetrabutylammonium acetate
MeCN	Acetonitrile
cm	Centimeters
FT-IR	Fourier-transform infrared
NCA	A-amino acid N-carboxyanhydride
HPLC	High performance liquid chromotography
mol/min	Moles per minute
[TBA][C_2S_6]	Tetrabutylammonium thioperoxydicarboxylate
PNPCHOO	Bis(triphenylphosphoranylidene)ammonium formate
NMR	Nuclear magnetic resonance
GC	Gas chromatography
$(PNP)_2SO_4H$	Bis(triphenylphosphoranylidene)ammonium sulfate
EPR	Electron paramagnetic resonance
18-crown-6	1,4,7,10,13,16-hexaoxacyclooctadecane
g	Landé g-factor
G	Gauss

Introduction

Chapter 1 – Adducts of Carbon Disulfide

1.1 Carbon Disulfide

Carbon disulfide (CS_2) is a triatomic, linear molecule, which at ambient temperatures and pressures is a highly volatile liquid. The molecule has no overall dipole moment because of its linearity, but due to differences in electronegativity the C=S bonds are polar. The electron density of the molecule is pulled toward the sulfur atoms, leaving them electron rich while the carbon center of the molecule is electron deficient. This allows the molecule to act as a Lewis base through the sulfur atoms and a Lewis acid through the carbon atom, much like carbon dioxide (CO_2), with which it is isoelectronic.

1.2 Transition Metal Complexes with CS_2

While here we will focus mainly on the on the formation of acid/base adducts with CS_2, it is worth briefly mentioning its interaction with metal centers as it highlights the molecule's status as both a Lewis acid and base. When introduced to metal compounds, CS_2 can either act as a chelating ligand through the terminal sulfur atoms[1] or as a π-complex via the carbon sulfur double bond.[2] Its first ionization energy is 10.1eV, making it a better electron donor than the isoelectric CO_2 that has a first ionization energy of 13.78eV, which is expected based on a comparison of their heteroatoms.[3] Oxygen is much more electronegative compared to sulfur and does not allow as much electron density to be transferred to the metal center. The chemistry of these complexes is incredibly diverse,

with research and applications branching into catalysis, polymers, molecular activation and more.[1]

1.3 Adducts of CS_2 with Lewis Basic Nitrogen

Leaving transition metal chemistry, it is logical to examine the interactions between CS_2 and amines. The two initially react to form a zwitterionic species via the nucleophilic attack on the central carbon atom by the lone pair of electrons on the amine[4]. This interaction is a prime example of CS_2 acting as a Lewis acid when in the presence of a stronger base. These species are unstable due to the lack of charge separation and will quickly go through some form of degradation. The most common course is the transfer of a proton from the amine to the terminal sulfur to form dithiocarbamates.[5-7] These dithiocarbamates are usually then deprotonated by another molecule of the original amine to form salts, though they may also stay protonated and will act as dithiocarbamic acids.

This highlights one feature of CS_2 adducts that will be seen a number of times through the introduction. While the sulfur atoms are not particularly strong bases in the neutral molecule, they do become much stronger once the adduct has been formed and a full negative charge is shared between them. Depending on the situation they can react in an intramolecular fashion, such as in the case of dithiocarbamate formation discussed above, or they will attack other molecules in the system.

Another case in which the sulfur atoms act as intramolecular bases is in the reaction of CS_2 with azides. The first observation of this reactivity dates back to 1921 when Brown and Hoel[8] performed a series of experiments with CS_2 and sodium azide.

While they theorized that the product produced in the reaction was azidodithiocarbamate, it was later shown by Lieber *et al.* (1951) that the true structure was sodium 1,2,3,4-thiatriazole-5-thiolate.[9] The formation of a five membered ring greatly increases the overall stability compared to that of other adducts and is initiated by one of the sulfur atoms acting as a Lewis base. The formal [2+3] cycloaddition starts with a nucleophilic attack on the central carbon atom of CS_2 which leads to the stable cyclic product shown in Figure 1.
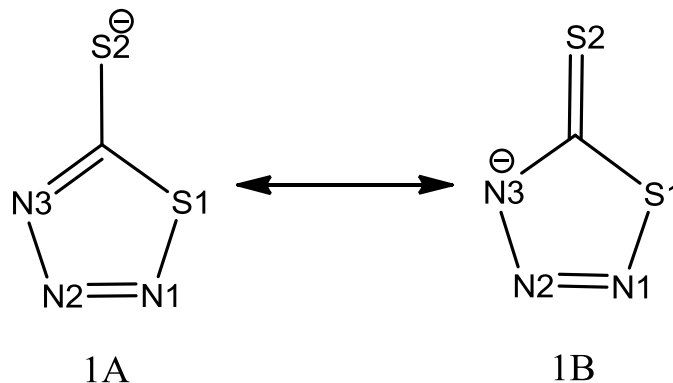
Figure 1: The two key resonance structures for the 1,2,3,4-thiatriazole-5-thiolate anion.

Despite the determination of the anion's structure, debate continued as to whether structure 1A or 1B was the largest resonance contributor, as well as whether the addition of electrophiles would happen at the exocyclic sulfur (S2) or the N3 position. While these are not the only resonance structures they were deemed to be the most stable. These debates were eventually settled when the crystal structures of sodium 1,2,3,4-thiatriazole-5-thiolate dihydrate and 5-benzoylthio-1,2,3,4-thiatriazole were reported by Perman and

Gleason in 1991.[10] Their results showed that the negative charge preferred to be on the sulfur atom (1A) and it was through this atom that reaction with electrophiles would occur. Since these initial discoveries, many additional thiatriazole anions and their derivatives have been synthesized and characterized.

1.4 Adducts of CS_2 with Phosphines

Taking one step further down the periodic table, it is not surprising that there are also examples of CS_2 forming adducts with phosphines. By the same mechanism as that with amines discussed above, the initial adduct formation produces a zwitterionic species. Such species were first isolated as crystalline solids by Hoffmann in 1880[11]. The difference for this type of phosphorus-containing compound, relative to the amine products, is that it is much more common for them to stay in their zwitterionic forms. These zwitterionic species can then be introduced as S,S-chelating ligands[12] onto other metal centers in a similar fashion to free CS_2 coordination to metals as mentioned above. In certain situations it is possible for them to function as η^1-σ donors,[13] through a single sulfur atom, or as η^1-π donors,[14] through the conjugated system. For less basic trialkylphosphines this is the only way that they can be isolated as they are not stable enough to be exist as pure compounds.
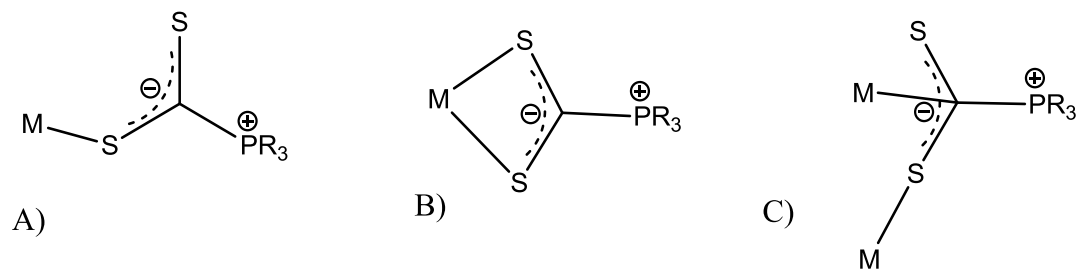
Figure 2: Structures of A) η^1-σ B) η^2-σ and C) η^1-π donating PR$_3$-CS$_2$ ligand.

1.5 Halogen and Pseudo-halogen Adducts with CS$_2$ and CO$_2$

The simplest adducts of CS$_2$ contain only a few atoms, namely those formed with halogens and pseudo-halogens. Very few complexes have ever been reported, and the information on those that have been is slim. In one report[15] it is stated that the reaction between tetrabutylammonium fluoride and CS$_2$ forms a dark red solution that the authors predict is the acid base adduct of fluorine and carbon disulfide (Figure 3A). The characterization is done only by UV and IR spectroscopy. The only other simple acid/base adduct known for CS$_2$ is cyanodithioformate, which in 1955 was shown to form from sodium cyanide and CS$_2$ by Bahr and Schleitzer[16] (Figure 3B). Both products were reported to decompose in air, changing from dark red crystals to yellow liquids, implying they are easily hydrolyzed or oxidized.

2A   2B
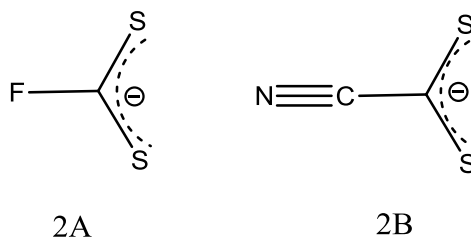
Figure 3: Known CS_2 adducts with halides or pseudo-halides

It is easy to understand why these two adducts would be the only ones reported if the area of halogen and pseudo-halogen adducts had a limited amount of research. Of the group, F^- and CN^- are two of the strongest bases, particularly when compared to atoms like bromine or iodine. They would therefore be the most likely to attack CS_2 and form bonds that were stable enough to be isolated, instead of immediately breaking down. Degradation, which does appear to be an issue, is also easily explained. While the strong bases are more likely to form bonds, the bonds are weak. This leaves the adducts open to hydrolysis or other forms of degradation, where the bases leave to form stronger bonds with other groups.

While examining the halide/pseudo-halide adducts of simple bases with CS_2 it is interesting to compare them with those formed with carbon dioxide. The first striking similarity is actually the lack of adducts that have been isolated and reported. The first CO_2 adduct to be discovered was the fluorocarbonate anion isolated in 1995 by Zhang *et al.*[17]. This adduct had been long predicted to exist through computational methods but its isolation and characterization were difficult. Formation of the adduct proved unfavorable under most conditions and it was incredibly vulnerable to hydrolysis. The only other known pseudohalogen acid/base complex of CO_2 is the cyanoformate anion isolated in

2014 by Murphy *et al.*[18] It was plagued by the same stability issues as the fluorocarbonate anion. These salts were both formed by the direct exposure of fluoro or cyano salts, with large, non-coordinating cations, to gaseous CO_2.

While the C–F and C–C bond lengths (1.367 and 1.480(9) Å, respectively) for fluorocarbonate and cyanoformate would not immediately imply weak interactions, there are other indications of how tenuous these bonds are. For one, both anions were hydrolyzed in the presence of even trace amounts of water. Also, while the C–C bond in cyanoformate is not particularly long, the C–O and C–N bonds of the anion are all much shorter than would usually be seen in an adduct. With these bonds being closer to the lengths of those in their constituent molecules (ions) it suggests that the anion is close to breaking down.

The lack of simple acid base adducts of CO_2, and the fragility of those that do exist, is due to a number of factors. The first main factor is the bending energy required for CO_2. To form an adduct with CO_2 the linear molecule must be bent, forcing the oxygen atoms much closer to each other than they were before. Due to the high electronegativity of oxygen this is difficult to do and requires a large amount of energy. The second factor is the lack of charge distribution available in the molecule once the adduct has been formed. For the larger species, such as in the example of the 1,2,3,4-thiatriazole-5-thiolate anion, the ability to create resonance structures stabilizes the molecule. For simple acid/base adducts such as the cyano- or fluorocarbonates there are very few atoms for the charge to be delocalized over, which leads to the molecule being much higher in energy and therefore much more likely to react or degrade. The common exception to this rule are carbonates and bicarbonates, the acid/base adducts of CO_2 with

hydroxide in both the protonated and deprotonated forms. These are unique in the fact that they are heavily stabilized in the solid phase by hydrogen bonding networks that is what makes them more stable than many of the other adducts. In the solution phase however they lose some of this hydrogen bonding and can allow them to be broken apart in certain situations.[19]

1.6 Adducts of CS_2 with Lewis Basic Oxygen

To move onto what will be the focus of this thesis, there are a few examples in the literature of CS_2 coordinating to basic oxygen atoms in molecules. One good example is the work done by Heldebrant *et al.*[20] in 2009 where they showed the coordination of CS_2 to deprotonated hexanol. The group 1,8-diazabicyclo[5.4.0]undec-7-ene (DBU) was used to deprotonate the hexanol, which produced an ionic liquid. When exposed to CS_2 the ionic liquid would turn a bright red colour, which was attributed to the formation of an *O*-alkylxanthate salt. The same reaction was not observed in solutions of CS_2 with only hexanol or DBU, which shows that on its own hexanol is not a strong enough base to form the adduct of CS_2. This does suggest a limit to the acidity of CS_2, particularly with an electronegative atom like oxygen, which is less likely to perform a nucleophilic attack if it is already neutral.

Another particularly interesting example of CS_2 coordination is from M. Isabel Cabaço *et al.* in 2014.[21] These authors combined CS_2 with 1-butyl-1-methylpyrrolidinium acetate ([BmPyrro][Ac]).[12] While the cation played no role in the reaction, the acetate anion reacted with CS_2 to form thioacetate, carbonyl sulfide (COS),

and CO_2 (Scheme 1). The group did not detect the presence of trithiocarbonate (CS_3^{2-}) through their standard methods, but because it shared a similar UV spectrum to their final reaction solution theorized that it was the cause of the dark red colour observed in the reaction. They did not propose a mechanism for CS_3^{2-} production, saying only that it is a side product generated in low concentration. While this is possible, when compared to the red colour observed with the hexanol and the fluorine adducts of CS_2, it is also possible that this colour is due to the acetate-CS_2 adduct being present in the solution.

$$[C_9H_{20}N^+][CH_3COO^-] + CS_2 \rightarrow [C_9H_{20}N^+][CH_3COS^-] + COS$$
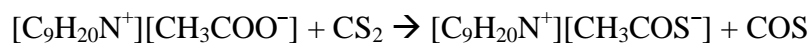
Scheme 1: Exchange reaction between 1-butyl-1-methylpyrrolidinium acetate and CS_2.

Cabaço *et al.* used DFT calculations to propose a reaction mechanism in which an adduct was formed between CS_2 and acetate, which once held together would exchange heteroatoms before breaking apart into thioacetate and COS. The CO_2 would then be evolved from molecules of COS that went through another exchange reaction with excess acetate anions.

Chapter 2 – Sulfur Dioxide as an Acid Gas

2.1 Acid gas properties of SO_2

As an acid gas, sulfur dioxide (SO_2) has a number of interesting properties that the carbon based acid gases (CS_2, COS and CO_2) do not have. While it is also triatomic, the pair of nonbonding electrons on the sulfur atom gives the molecule a bent structure. This leads to the molecule having an overall dipole moment, unlike the linear acid gases, which leaves the sulfur atom electron deficient while the oxygen atoms are electron rich. It is slightly counterintuitive that the atom with the lone pair of electrons would carry a partially positive charge, but the reasoning can be seen in the resonance structures of SO_2. Sulfur is much less electronegative than oxygen and therefore will allow electron density to be pulled away from it. These differences make SO_2 a better candidate for adduct formation than the carbon-based acid gases. With the molecule already in a bent conformation, the energy required for adduct formation is significantly decreased. As well, the permanent dipole makes the molecule more reactive toward nucleophilic attack.
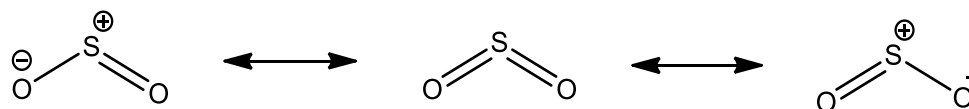
Figure 4: Resonance structures of SO_2.

2.2 Halogen and Pseudo-halogen Adducts with SO$_2$

Due to these advantages, interactions of halides or pseudo-halides with SO$_2$ have been the focus of more research than the other gases discussed in this review. However, there is still much left to discover. Adduct formation is based on the nucleophilic attack of the Lewis acidic center by a Lewis base. Again, like the other acid gases, the adducts with the strongest bases were the first to be isolated due to the stronger bonds that are formed. SO$_2$ does form a few adducts which have not yet been isolated with the other gases: so far adducts with [F$^-$][22], [CN$^-$][23], [N$_3$$^-$][24], [Cl$^-$][25] and [I$^-$][26] have been reported.

Fluorosulfite was the first of the simple acid base adducts of SO$_2$ to be isolated (1953). Seel *et al.*[22] went on to publish a number of papers in the following decade on the subject.[27,28] The synthesis involved the reaction of Group 1 fluoride salts, as well as tetramethylammonium fluoride [(CH$_3$)$_4$NF], with SO$_2$ to give the sought after FSO$_2$$^-$ anion. While a number of different structures were studied, there was no definitive geometry identified for the compound until a 2001 publication by Lork *et* al[29]. This was only after a number of others had attempted to solve the structure with little success due to its high level of disorder. The crystal structure followed the general trends of SO$_2$X$^-$ (X=halogen) anions that will be discussed below.

The first crystal structure reported was for SO$_2$I$^-$ by Eller and Kubas[26] in 1978. The salt was prepared by bubbling SO$_2$ though a solution of triphenylbenzylphosphonium iodide, [BzTPP]I, in warm acetonitrile to give the bright yellow crystals that were determined to be [BzTPP][SO$_2$I] using X-ray crystallography. The structure showed a pyramidal geometry for the anion with I-S-O angles of 102.1(5) and 105.7(4)°. This

geometry is to be expected, as it allows for the maximum attraction between the halogen and sulfur while keeping the iodide well separated from the oxygen atoms. Unsurprisingly then, these characteristics will trend through nearly all of the known structures.

$$X \longrightarrow S \overset{\overset{\displaystyle O}{\diagup}}{\underset{\diagdown}{\underset{\displaystyle O}{}}} \ominus \quad \sim 100°$$
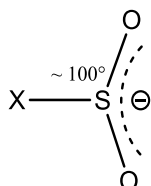
Figure 5: General structure of the SO$_2$X$^-$ anion where X=F, Cl, I, CN or N$_3$.

The geometries of the next three anions to be isolated, SO$_2$Cl$^-$ (1994[25]), SO$_2$CN$^-$ (1999[23]) and SO$_2$N$_3$$^-$ (2002[24]) also follow these trends. The azido- and cyano- anions were again isolated after the direct exposure of their salts to SO$_2$; however, in these cases the syntheses were performed using liquid SO$_2$ because neither of the adducts were stable at room temperature, and even below that they would decompose within a day. This does show that unlike the sulfur atoms of CS$_2$, the oxygen atoms of SO$_2$ are much less likely to act as Lewis bases once the negative charge of the adduct is shared between them which leads to more stable adducts. This can be explained by the much higher electronegativity of the oxygen atoms, meaning that they are more stable with a negative charge and less likely to give up their extra electrons.

The method reported for the synthesis of SO$_2$Cl$^-$ by Kuhn *et al.* was by far the outlier of the group.[25] The adduct was prepared by reacting imidazol-2-ylidene (*i*-Pr$_2$Imes) with sulfuric chloride (SO$_2$Cl$_2$) at -78°C in diethyl ether to give the [*i*-

Pr$_2$ImesCl]SO$_2$Cl product. The chemistry and geometry of the anion similar to the previously observed adducts. As Cl$^-$ is a comparatively weaker base that anions like CN$^-$ and F$^-$, it is not thermodynamically favorable for an adduct to form from direct exposure of an Cl$^-$ salt to SO$_2$. This is why to synthesize the SO$_2$Cl$^-$ adduct Kuhn *et al.* started from SO$_2$Cl$_2$ and then used the energy from the formation of [*i*-Pr$_2$ImesCl]$^+$ to achieve the SO$_2$Cl$^-$ adduct.

2.3 SO$_2$ as a Reducing Agent

SO$_2$ is an incredibly versatile molecule that has many different uses. It is possible for SO$_2$ to act as both a reducing and as an oxidizing agent as sulfur can exist in both higher oxidation states (such as sulfuric acid) and in lower oxidation states (such as in hydrogen sulfide). However when looking at the common applications of SO$_2$ there are abundant examples of SO$_2$ acting as a reducing agent, such as in the paper and pulp, wine, and water treatment industries. On the other hand there are precious few examples where its role is that of an oxidizing agent. In situations where SO$_2$ is reduced, the use of extreme temperatures, high pressures, catalysts or electroreduction are usually required.

The reactions in which SO$_2$ acts as a reducing agent are favorable enough that it is possible to find numerous examples of this reactivity in industrial applications. One common use is for the removal of chlorine from treated water.[30,31] Chlorine is commonly used to disinfect water, but it also is incredibly toxic toward plant and aquatic life that it comes into contact with. Therefore any excess chlorine must be removed from water before it can leave a waste treatment plant. The excess chlorine can be in two forms,

HOCl which is commonly referred to as "free chlorine" or as inorganic chloroamines in the form of NH_2Cl. One way of removing both types is by bubbling SO_2 through the water, or by adding in sulfate (SO_4^{2-}) or sulfite (SO_3H^-) salts to the water. Both forms of the chlorine will be reduced by the sulfur species and be released as chloride, which is a naturally occurring anion and relatively harmless to the environment.

$$1)\; SO_2 + H_2O \rightarrow HSO_3^- + H^+$$

$$2)\; HOCl + HSO_3^- \rightarrow SO_4^{-2} + Cl^- + 2H^+$$

$$3)\; SO_2 + NH_2Cl + H_2O \rightarrow Cl^- + SO_4^{-2} + NH_4^+$$

Scheme 2: Reaction process in which SO_2 removes chlorine as both free chlorine (2) and as inorganic chloroamines (3).

The reducing capabilities of SO_2 also make it a powerful antimicrobial agent, which has led to its common use in the wine and cider industries.[32] When added to wine SO_2 is usually converted to sulfites by the water in the system, and from that state can act as a reducing agent towards oxidizing enzymes. This is usually done after the fermentation process of the wine making has been completed, which allows the SO_2 to help control the growth of unwanted bacteria that would spoil the wine. This application has been in common use for hundreds of years, with the oldest known reports dating back to the Romans, who would sometimes burn sulfur candles in the wine barrels before shipping.[33]

2.4 SO$_2$ as an Oxidizing Agent

One of the most common reactions in which SO$_2$ acts as an oxidizing agent is the Claus process.[34] This process was patented in 1883 by Carl Claus as a way to remove elemental sulfur from sulfur containing gases, whether produced by the petroleum industry or found in natural gas. It has become the industry standard for the desulfurization of gases. The first step in this multistep process is the combustion of a highly concentrated H$_2$S gas to produce SO$_2$, H$_2$O, elemental sulfur and some unreacted H$_2$S. Under these conditions SO$_2$ can then act as an oxidizing agent towards any remaining H$_2$S to form elemental sulfur and water, though the reaction does not go to completion. Once the pure sulfur and water have been separated out by condensation, the mixture of gases is then passed over a bed of activated aluminum (III) or titanium (IV) oxide.

These metal oxide catalysts are surface active and reduce the sulfur dioxide through oxide vacancies.[35] The first step in this process is having both SO$_2$ and H$_2$S reversibly bond to the surface. Once bonded, single hydrogens from H$_2$S can be transferred to nearby surface active sites. These now activated hydrogens can then act to reduce other nearby SO$_2$ molecules to produce elemental sulfur and water. The newly formed atoms of elemental sulfur go on to combine with others, either from reduced SO$_2$ or SH molecules that were reduced by the water molecules, to form different allotropes with the most prevalent being S$_6$ and S$_8$. These types of transition metal oxide catalysts

are commonly used in a number of SO_2 reduction reactions, including its reduction to elemental sulfur by carbon monoxide.[36]

$$2NaCOOH + Na_2CO_3 + 4SO_2 \rightarrow 2Na_2S_2O_4 + H_2O + 3CO_2$$
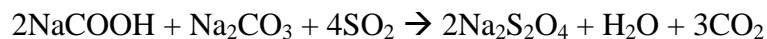
Scheme 3: Reaction equation for the industrial production of dithionite.

Another prominent industrial reaction that involves the reduction of sulfur is the production of dithionite (also known as hydrosulfite) salts. Dithionite salts, particularly sodium dithionite, are used as strong reducing agents in the pulp and paper industry.[37] One of the most common manufacturing techniques is to react sodium formate ($NaCO_2H$) and sodium carbonate (Na_2CO_3) with SO_2 under elevated temperatures and pressures.[38] The reaction, as shown in

Scheme 3, results in the reduction of SO_2 and carbonate and the oxidation of formate. It is theorized that the initial redox reaction is between SO_2 and NaCOOH which gives off CO_2 and hydrogen. The hydrogen then goes on to reduce the carbonate salt to give water and CO_2. While this hypothesis does seem reasonable, there have been no definitive mechanistic studies on this reaction.

2.5 Chemistry of the $SO_2^{\bullet-}$ Radical Anion

Dithionite is also involved in one other type of SO_2 chemistry. Under most conditions, the dithionite anion exists in equilibrium with two molecules of the $SO_2^{\bullet-}$ radical anion.[39,40] The radical anions are formed by the homolytic cleavage of the S-S

bond in dithionite, and while are not favored by the equilibrium, they do exist in small proportions.
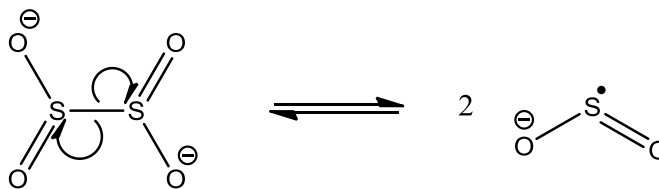
Scheme 4: Homolytic cleavage of dithionite to $SO_2^{\bullet-}$.

Research into these radical species has determined that they can also be produced under acidic conditions in which SO_2 is reduced to the radical, or by pulse radiolysis; both methods have been used to study the species.[41,42,43] The dithionite system is the simplest way to study the radical anion of SO_2; it can also be produced by electromagnetic radiation, but with much more effort than with dithionite. The ease of the homolytic cleavage has also led to dithionite being used as a radical initiator for a number of reactions. Under normal conditions it is water stable and can easily be applied to different reactions including radical polymerizations.

When $SO_2^{\bullet-}$ is produced through means other than the cleavage of dithionite, there has been some debate in the literature about the reaction intermediates. The debate stems from the production of a distinct dark blue colour when the SO_2 radical anion is produced. It was initially thought that this blue species was the product of $SO_2^{\bullet-}$ and SO_2, the blue $S_2O_4^{\bullet-}$ radical, a species that had been reported by Gardner *et al.*[44]. This proposal was later proved incorrect by Potteau *et al.*[45], when they identified the species as $S_4O_8^{2-}$, the dimer of the previously studied radical. In the same paper they also identified another

distinct red species, $S_3O_6{}^{2-}$, which was most likely, at room temperature, the product of $SO_2{}^{\bullet-}$ and $S_2O_4{}^{\bullet-}$. This shows that like many radical reactions, a wide range of species can be and are produced if there is not strict control over the reaction.

Results & Discussion

Chapter 3 –Reactivity of CS_2 with the Acetate Anion

3.1 Computational Study of Adduct Formation

Before experimental studies were started, an initial theoretical investigation into the bonding energies of acetate to carbon based acid gases was performed. The goal was not to predict the exact energy in the system, but rather to be able to determine which gas the anion would be the most likely to bond to. The expectation was that by replacing oxygens sequentially with sulfur atoms, the bending energy of the gas would decrease and therefore the adduct would be more likely to form. The computations were done using Spartan '14[46] at the B3LYP[47,48] level of theory, using the 6-31G* basis set, in a vacuum.

Table 1: Summary of bonding energies for the adduct formation between the acetate anion and carbon based acid gases

Acid Gas	X-C-X Angle	C-O (acetate to gas) bond length	Energy of adduct formation (au)	Energy of adduct formation (kJ/mol)
CO_2	140.69°	1.664 Å	-0.026450	-69.44448029
COS	132.22°	1.498 Å	-0.032805	-86.12953406
CS_2	131.43°	1.446 Å	-0.037007	-97.16188590

The data in Table 1 show an evident trend that matches the expected results. Not only is the bonding energy for CS_2 the lowest but the bond length between the gas and the anion is the shortest and the X-C-X angle is the closest to the 120° angle of a perfect trigonal planar molecule. These trends support the hypothesis that there will be chemistry

observed between acetate and CS_2 that would not be observed with CO_2 due to the less favorable thermodynamics.

3.2 Screening for Reactivity with CS_2

Before focusing on a particular anion to study, a general screening was done to observe the reactivity of several selected anions with CS_2. The salts chosen all had large, non-coordinating cations and small "naked" anions. Each of the chosen salts was dissolved in a minimal amount of acetonitrile (MeCN) before placing each vial in a desiccator and adding dry CS_2 to each vial. When the salts were exposed to CS_2 in the solution phase, the following observations were made (Table 2):

Table 2: Summary of observations from screening for the reactivity of salts with CS_2

Salt	Observations
Tetrabutylammonium acetate	Turned dark red within a minute of addition, turned yellow after a few hours
Tetrabutylammonium benzoate	Turned red after 10 minutes then yellow overnight
Tetrabutylammonium bromide	No reaction was observed
Tetraphenylphosphonium iodide	No reaction was observed
Tetrabutylammonium fluoride	Turned dark red immediately upon addition and stayed red for 24 hours before turning yellow
Tetrabutylammonium cyanide	Turned yellow to brown to black upon addition and stayed black

The observations show that there is definite reactivity between some of the halide and pseudo-halide anions and the CS_2. The red colour observed is very similar to the observations made by other groups[15,20,21] in which the formation of an adduct of CS_2 and

a strong base gave a dark red solution. In one study[15] the base used was fluoride, while in another[19] it was 1,8-diazabicyclo[5.4.0]undec-7-ene (DBU). With such vastly different bases, it is most likely that the red colour comes from either the bent CS_2 fragment of the molecule, the base-CS_2 bond or from the process of the adduct formation itself. If this is correct, it would imply that the carboxylates also initially form adducts with CS_2, since the rapid colour change to dark red is also observed in their reactions. However, the subsequent change to a yellow colour suggests that these then somehow change or fall apart over time. To continue the investigation, tetrabutylammonium acetate (TBAA) was chosen for further study.
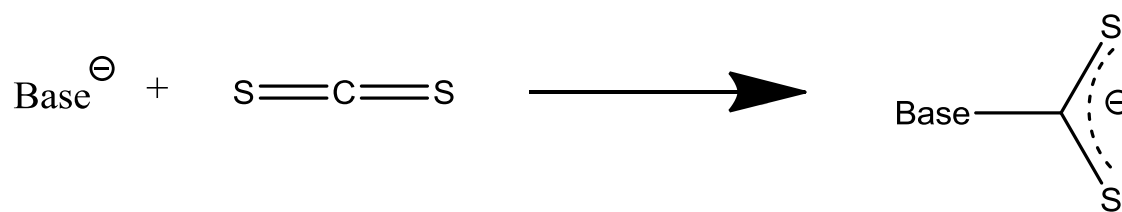
Scheme 5: General structure of acid base adducts of CS_2.

3.3 Characterization of Products from TBAA and CS_2

The next step in the study was to repeat the small scale reaction on a larger scale and allow the products to crystallize. When repeated, the same colour changes were observed upon the addition of CS_2. As the solvent evaporated the remaining solution became much more viscous, most likely due to unreacted CS_2, and after two days long needle crystals grew from the reaction mixture. The crystals were clear and colourless though the viscous solution around them remained dark yellow. A single crystal was analyzed using X-ray crystallography and found to be tetrabutylammonium thioacetate.
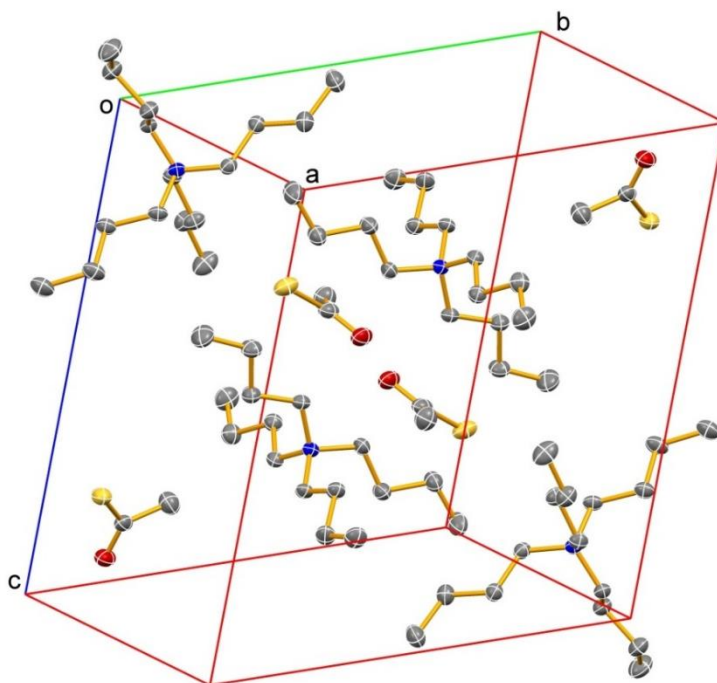
Figure 6: The crystal packing structure of tetrabutylammonium thioacetate. Hydrogen atoms have been removed for clarity. Thermal ellipsoids are drawn at the 50% probability level.

This was not the expected structure, based on the adduct observed by Heldebrant *et al.*[20] and the acid/base adducts prepared with $[F^-]$[15] and $[CN^-]$.[16] However, similar results had been reported by Cabaço *et al.* in 2014.[21] These authors introduced CS_2 into the ionic liquid, 1-butyl-1-methylpyrrolidinium acetate and produced a thioacetate anion and carbonyl sulfide (COS) gas. In this reaction they also observed the dark red colour typical of acid base adducts of CS_2. Such an exchange reaction had only ever been reported in an ionic liquid; because of the isolation of the thioacetate anion it was reasonable to test the current reaction mixture for the presence of COS. To do this, an *in situ* ReactIR study of the reaction was carried out in an acetonitrile solution. A larger scale reaction was used for this study, with the TBAA being dissolved in acetonitrile for the initial scans and then CS_2 being added to the reaction flask. While COS is a gas at

room temperature, it is soluble enough in MeCN that it is detectable in solution using the ReactIR.
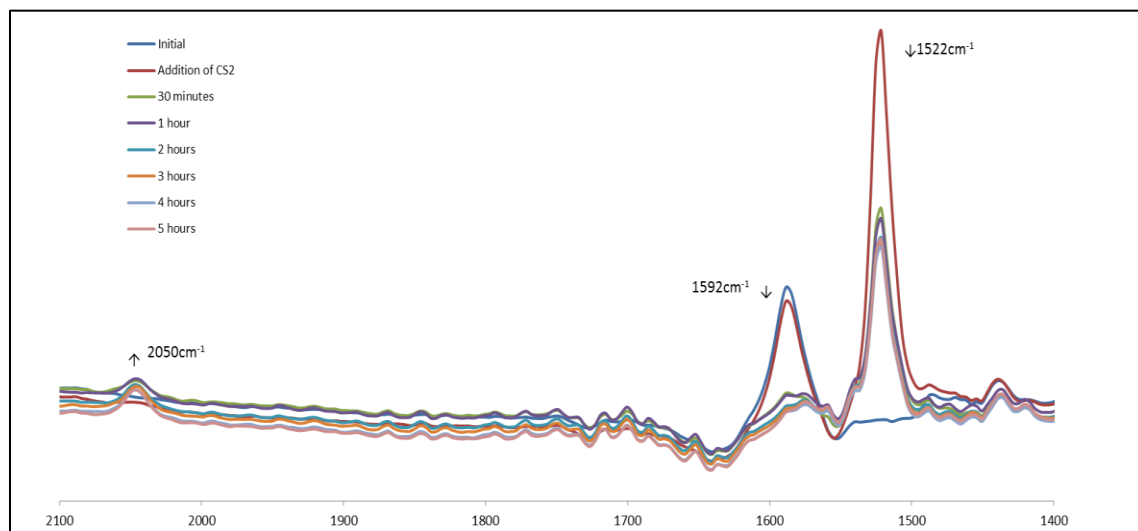
Figure 7: Infrared spectra from the reaction between TBAA and CS$_2$, monitored *in situ* using ReactIR.

The time resolved, overlaid spectra in Figure 7 show three peaks that have undergone significant changes. There is a decrease in the peak heights at both 1522cm^{-1} and 1592cm^{-1}. These peaks represent the asymmetric stretch of CS$_2$, ν_{as}(CS$_2$),[49] and the carbonyl stretch of TBAA, ν(CO),[50] respectively. It is reasonable that they would drop as the starting materials are consumed in the reaction. The third change is in the appearance of a peak at 2050cm^{-1}, which increases in intensity. This peak is assigned to the asymmetric stretch of COS, ν_{as}(COS),[51] a gas that is produced in the reaction.

The observation of COS confirmed the proposal that the acetate anion and the CS$_2$ gas were exchanging heteroatoms in the reaction. In their article Cabaço *et al.* reported a

computational study of the mechanism for this reaction. They found it to be very similar to the oxidation mechanism of CS_2 to COS by water that has been studied computationally by Ling *et a.l*[52] The mechanism (Scheme 6) starts with a nucleophilic attack at the carbon center of CS_2, which shifts the negative charge of the acetate onto one of the sulphur atoms. This sulphur atom then attacks the carbonyl carbon on the acetate, breaking the bond to its original carbon. In the same step the electrons from the single bond between the central acetate carbon and the oxygen are shifted to the newly formed carbonyl sulfide, completing the transfer.
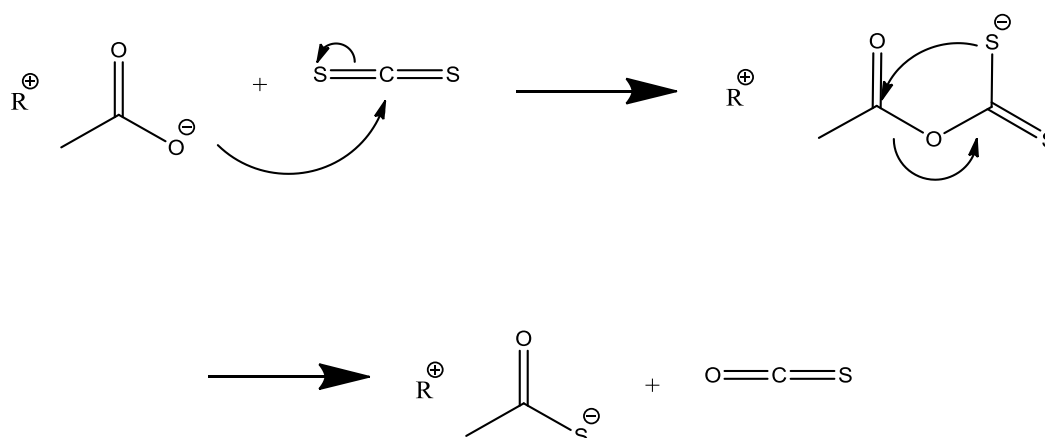
Scheme 6: Proposed mechanism for the exchange of oxygen and sulfur.

When looking at the changes in the IR spectra for this reaction, there was not a significant difference observed from the time when the CS_2 and acetate peaks started to drop and when the new COS peak became observable. This fits well with the computational study that Cabaço *et al.* performed, which predicted that the initial adduct formation would have the highest energy barrier with the step requiring 18.5 kcal/mol

with the next highest step only requiring 10.6 kcal/mol.. Therefore once that had occurred, the exchange step would rapidly occur to produce the observed COS.

3.4 Solid-Gas Reaction of TBAA and CS_2

As the main sources of CS_2 in the atmosphere are volcanic gases[53] and industrial pollution,[53] the introduction of CS_2 as a gas into the reaction was explored. Reactions often occur more readily in solution than in the solid phase, as it usually requires much more energy for reaction to occur between solid products, or a much longer reaction time. This is due to the strong intermolecular (interion) forces and highly limited movement in the solid phase compared to the relatively free movement in the liquid phase.

The reaction was performed in a gas cell with NaCl salt plates at the ends. This allowed FT-IR measurements to be taken of the atmosphere above the reaction. A small portion of TBAA was placed along the bottom of the chamber before it was evacuated. The chamber was then filled with a mixture of N_2 and CS_2 gases and a series of IR scans were taken over time. It was immediately apparent that a reaction had taken place as the solid turned bright red upon the addition of the gas; it faded to orange/yellow over time.

The time resolved IR spectra of the atmosphere clearly show the relative increase in the intensity of the asymmetric stretching peak of COS compared to the intensities of all three of the peaks attributed to the CS_2 gas. This shows that adduct formation is occurring even in the solid state and that from the adduct the exchange mechanism can still proceed.

Similar results were not obtained when the reaction was carried out with sodium acetate. It is theorized that with a smaller cation, such as sodium, the electrostatic attraction would be stronger due to the charge density. This would make the salt more stable than one with a large, non-coordinating cation, and therefore make adduct formation less thermodynamically favorable. The failure of the reaction to begin would explain why no COS gas was detected, as well as why no colour change was observed to indicate that the adduct was being formed.
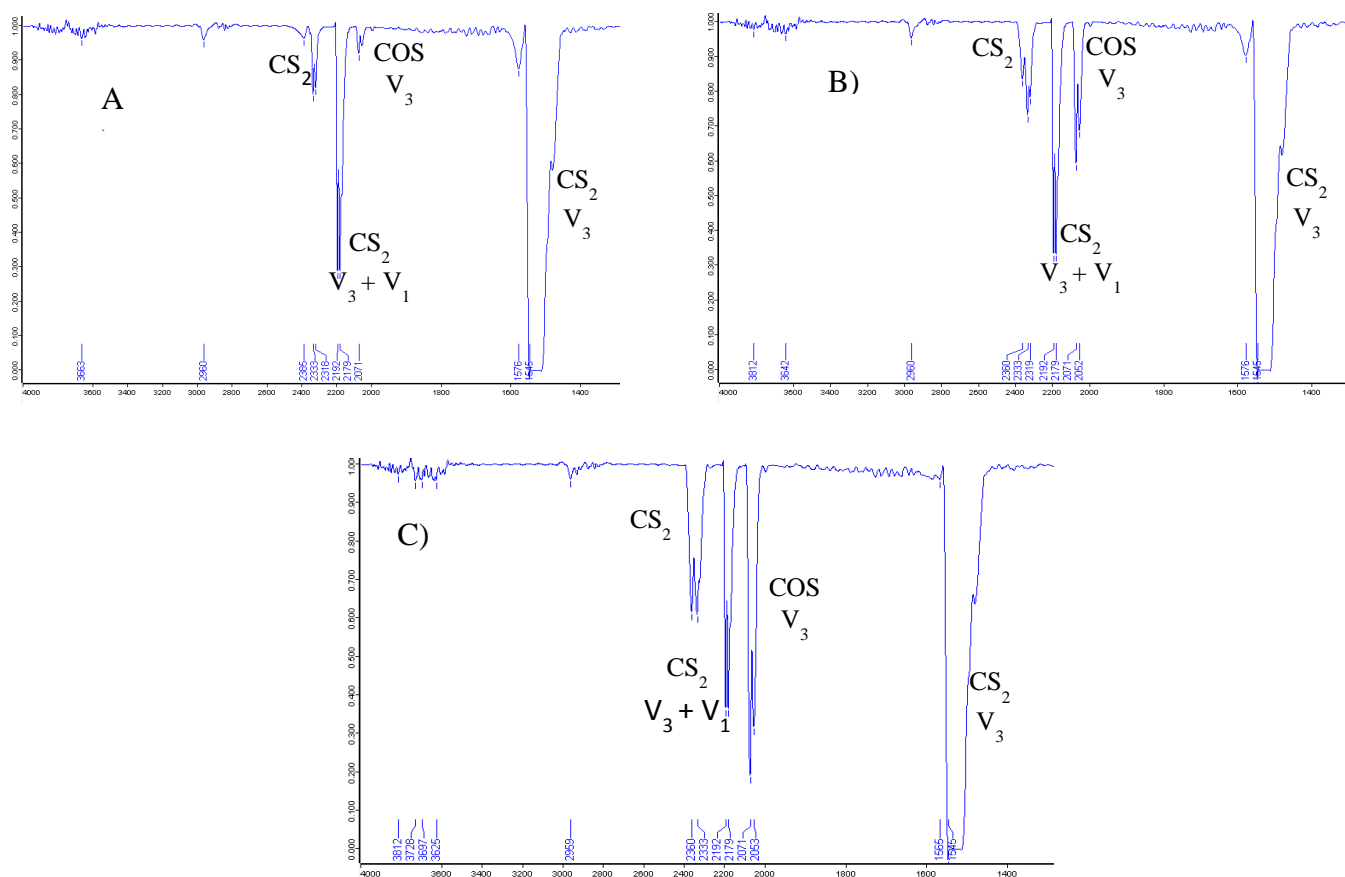
Figure 8: FT-IR spectrum of the atmosphere above the reaction of solid TBAA and CS2 at A) 2 minutes B) 2 hours and C) 20 hours

3.5 Kinetics Study

While our observations fit well with the proposed mechanism shown in Scheme 6, there was no quantitative experimental evidence to support the theory. To test whether or not the proposed mechanism was viable, a kinetics study was performed on the solution phase reaction. By changing the concentration of one reactant while keeping the other one constant, it is possible to determine the effect the concentration of the reagent has on the rate of the reaction. If a reactant's concentration has an effect on the rate, it means that its concentration appears somewhere in the rate law of the reaction, which in turn means that the reactant being measured is part of the rate determining step of the reaction. The mechanism supported herein says that the rate determining step, the one predicted to have the highest energy, is the formation of the adduct between the acetate anion and CS_2. If this is true, then the concentration of both molecules should impact the initial rate of the reaction.

With *in situ* IR the rate of disappearance of the acetate carbonyl peak was monitered over the course of the reaction. The same experimental procedure was followed as that used to detect COS, except the amounts of TBAA and CS_2 were varied. To overcome the fact that only relative peak heights were measured, the percentage change in peak height between the start and end of the experiment was used to calculate the moles of acetate which reacted. This was monitored over the first 3 minutes after the addition of CS_2 to the reaction vessel. The assumption was made that all of the added acetate reacted, as CS_2 in excess for all of the trials.

Table 3: Summary of the initial rates for the kinetics study

Run	Moles of TBAA	Moles of CS_2	Initial Rate (mol/min)
A	0.00199	0.01106	3.91562E-06
B	0.00209	0.00666	2.90438E-06
C	0.00202	0.00323	1.77363E-06
D	0.00106	0.00676	1.59906E-06
E	0.00050	0.00679	4.91692E-07

When the rates of each reaction are compared to the moles of reactant present, it can be seen that higher concentrations of each of the reactants produce a higher initial rate. While no more quantitative insight about the rate law can be pulled from this data, it does support the hypothesis that both molecules are involved in the rate determining step. This is further support for the mechanism proposed by Cabaço *et al.* which predicted the rate determining step to be adduct formation, which requires the involvement of both molecules.

To test the resilience of the reaction, another series of experiments was performed. The first step was to dissolve TBA in acetonitrile and add an excess of CS_2 in a container exposed to the atmosphere (moisture). The characteristic colour changes were observed in this reaction, however, when the solvent from this solution was allowed to evaporate, crystals were isolated. These were found to be TBAA solvated with acetic acid. A similar lack of reaction was seen both when an aqueous solution of TBAA and when concentrated acetic acid were reacted with CS_2. However in these reactions no colour changes were observed and no solids were ever isolated.

There are two possible interpretations for these results, either (i) the reaction did occur and then the product was hydrolyzed or (ii) the water interfered with the mechanism preventing the reaction from occurring. Both of these explanations are plausible based on the mechanism that was proposed in Scheme 5. In studies of the thioacetate anion, it has been shown that that the protonation occurs at the sulfur atom.[55] This allows the protonated acid to be easily hydrolyzed as HS^- is a better leaving group compared to HO^-. If the water was to reach the acetate first it would easily protonate the carboxylate to give acetic acid. If the proposed mechanism is correct, and the first step is the nucleophilic attack by the carboxylate on the CS_2 center, the protonation of the carboxylate would greatly decrease the nucleophilicity of the oxygen and therefore slow down the reaction to the point of it not occurring. It is most likely that, in the case of the first experiment where the colour changes were observed, the exchange reaction did occur and then the products were hydrolyzed. In the aqueous solutions, where no colour changes were observed, however, it is much more likely that the exchange reaction never occurred due to the lack of nucleophilicity of the oxygen. Overall, these observations tell us that for the reaction to occur the environment must be dry and alkaline to avoid protonation as well as hydrolysis of the final product.

The production of COS from a simple and fast reaction has interesting implications in the area of prebiotic chemistry. There are a few reasons to move to this type of environment when looking at the implications of the reaction. First, volcanic gases played a large role in the atmosphere of prebiotic Earth, and one of the gases produced was CS_2. This also means that the atmosphere was generally reducing, instead of the generally oxidizing atmosphere that now exists.[56] Simple carboxylic acids were

also common on prebiotic Earth, with acetate being produced by a single methylation step from CO_2.[57]

COS also has a rather interesting chemistry when it is in contact with amino acids. Studies have shown that COS will react with amino acids to form α-amino acid *N*-carboxyanhydrides (NCAs) under relatively mild conditions.[58] NCAs are cyclic species that present an activated version of the amino acid for condensation. This is important because under normal conditions the formation of polypeptides is unfavorable. To start with, amino acids must be in their neutral forms for the condensation reactions to occur, which in aqueous conditions is uncommon. On top of that, the actual condensation reaction is not thermodynamically favorable, meaning that when the hydrolysis of polypeptides is factored in there is usually no net reaction.
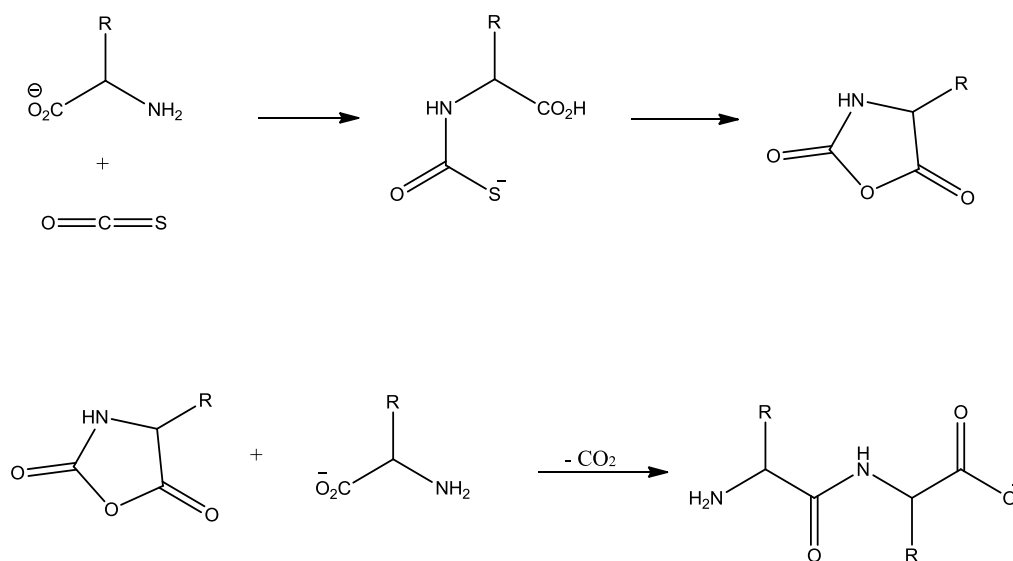
Scheme 7: The formation of an NCA and its reaction to form a dipeptide.

Studies have shown that COS will react with amino acids to form NCAs under relatively mild conditions. Further studies have also shown that the NCAs created from

COS will go on to form di- and tri-peptides even in aqueous solutions. One such paper by Leman *et al.*[58] showed that by simply bubbling COS gas through an aqueous solution of amino acids with a basic buffer, dipeptides could be isolated by reverse phase HPLC. With the addition of $[K_3Fe(CN)_6]$ to aid in the removal of the thiolate anion from the initial COS-amino acid adduct, traces of chains as large as hexapeptides were observed. The question that still remains is one of concentration. Most studies using NCAs introduce a high concentration of the activating molecule, which in the conditions of prebiotic earth may actually not have been available.

There is evidence of COS being produced on prebiotic Earth, but the reaction shown in this work has the advantage of producing a high local concentration of the gas compared to that found in the general atmosphere. A large problem in theories of abiogenesis is dilution. With most of the biologically active molecules being dispersed throughout the atmosphere or ocean, forming a high enough concentration of all of the necessary molecules close together would have been difficult to achieve. A reaction that produced COS would create a higher local concentration near any possible amino acids present, unlike volcanoes which would have most likely had their COS diffused throughout the atmosphere before it could reach any reactive substrate.

3.6 Isolation of Thioperoxydicarbonate

In one particular run, in which TBAA was dissolved in water and CS_2 was added, a completely different product was isolated. This reaction was done under a nitrogen atmosphere, and within the first 3 hours the solution changed from clear and colourless to a faint brown colour. After being left to stand overnight in a closed container, the solution

had darkened further and orange needle crystals had precipitated out of the solution. X-ray crystallography showed they were tetrabutylammonium thioperoxydicarbonate ([TBA][C_2S_6]).

Though at this point in our research we have not been able to reproduce this reaction, a few examples of the $C_2S_6{}^{2-}$ anion have been reported in the literature. [60,61, 62] The synthetic method is usually based on the reaction of trithiocarbonate ($CS_3{}^{2-}$) with CS_2 to produce the thioperoxydicarbonate anion. Surprisingly, these crystals are stable in an aqueous environment. They have certain applications as pesticides as they will slowly break down to release CS_2. It is most likely that there was some amount of unknown contaminant in the reaction flask that led to our isolation of this product, which would also explain the difficulty reproducing it.
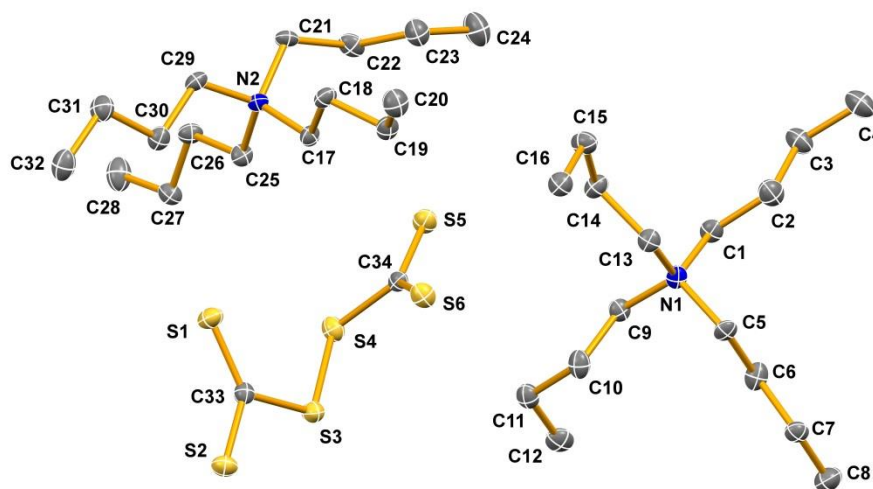
Figure 9: Crystal structure of [TBA]C_2S_6 Hydrogen atoms have been removed for clarity. Thermal ellipsoids are drawn at the 50% probability level.

In terms of my research, this reaction shows that the production of the thioacetate anion, along with the corresponding production of COS, is not favored in water even under an inert atmosphere. Thioperoxydicarbonate does however show a strong similarity to the polythionites that will be discussed in the next chapter, as well as potentially acting as a way of protecting CS_2 from oxidation.[62] CS_2 can be oxidized to CO_2 relatively quickly by water, which does involve a short period of time spent as COS. With thioperoxydicarbonate being water stable, it could protect the molecule until it was in an environment in which it could be released to form a high local concentration of COS through reaction with acetate, and be available as an amino acid coupling agent.

Chapter 4 – Reactivity of SO$_2$ with the Formate Anion

4.1 Screening of Salt Reactivity with SO$_2$

We next shifted the focus to the study of another acid gas, sulfur dioxide (SO$_2$). The initial goal of isolating an acid/base adduct with a carboxylate anion was still in place. SO$_2$ has a bent structure due to its lone pair of electrons on the central sulfur atom, a feature not present in CS$_2$. This lowers the bending energy required to form the initial adduct. Overall, this points toward SO$_2$ being more likely to form adducts, which has been shown in the literature. There are many more reported XSO$_2$⁻ structures than those of [XCS$_2$⁻] or [XCO$_2$⁻].[22-26] With the observations taken from the earlier experiments, however, we knew to also keep watch for other types of reactivity.
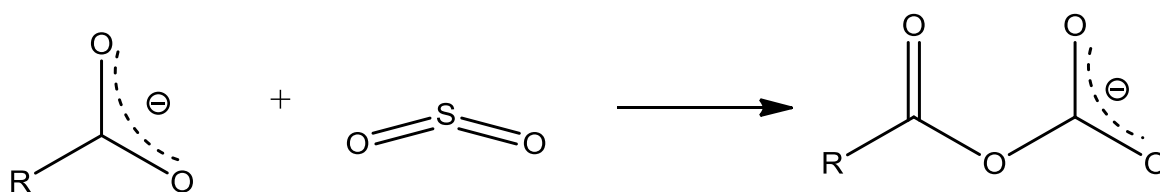
Scheme 8: Acid/base adduct of SO$_2$ with a carboxylate anion.

The initial screening for reactivity was done in much the same manner as the experiments with CS$_2$. Samples of the same salts as in the screening for CS$_2$ reactivity, along with bis(triphenylphosphoranylidene)ammonium formate ([PNP][CHOO]), were dissolved in a minimal amount of acetonitrile. The vials were placed in a vacuum desiccator along with toluene, to act as a counter solvent, and Drierite. The desiccator was then evacuated and filled with an SO$_2$ atmosphere. Care was taken to keep the environment as dry as possible and sealed from the ambient atmosphere, to avoid the

oxidation of SO_2 to sulfate or sulfuric acid, all of which prevent adduct formation from occurring.

In this case only one of the salts showed a visual sign of reaction. The solution of [PNP][CHOO], which had been prepared through the metathasis of bis(triphenylphosphoranylidene)ammonium chloride and sodium formate, immediately turned an opaque dark blue colour upon the addition of SO_2. This slowly faded to green and finally to transparent yellow over the span of two hours. The initial appearance and then subsequent change of colour was similar to what had been observed with CS_2 and the carboxylates. This led us to believe that an adduct was being formed first and then somehow reacting further or degrading.
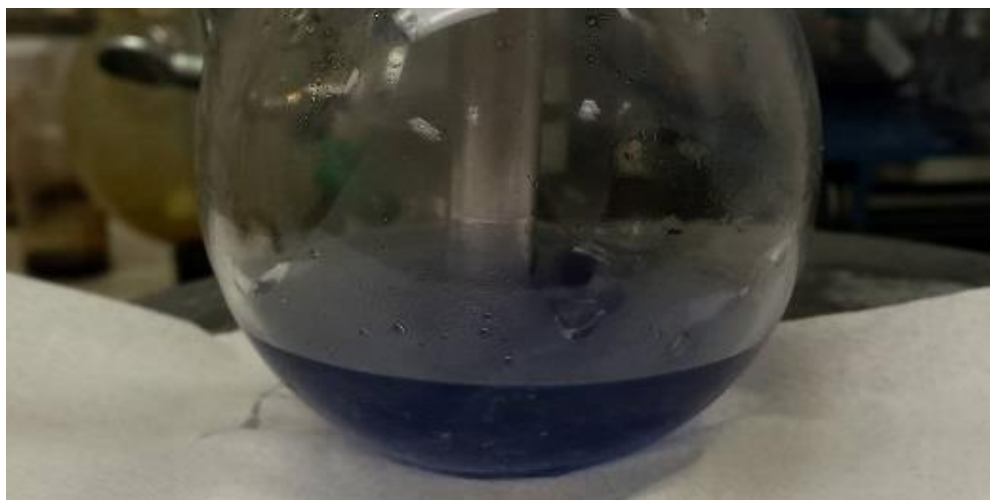

Figure 10: Dark blue solution phase of the reaction between SO_2 and [PNP][CHOO].

4.2 NMR Analysis of PNP[HCOO] and SO$_2$

The reaction was re-run on a larger scale using Schlenk techniques and the same colour changes were observed. Upon the addition of the SO$_2$ the flask gave off a significant amount of heat, becoming warm to the touch. Between the rapid appearance of the colour and the exothermic nature of the reaction, it was obvious that the reaction taking place was very thermodynamically favorable. When the ^{1}H NMR of the sample was run, however, the peak corresponding to the proton of the formate was almost completely gone, and it had not been replaced by any other protons in the system. This, along with the results from a literature search showing that the blue colour is characteristic of the dimer formed by the SO$_2$•$^-$ radical anion,[45] lead us to believe that a different type of reaction was occurring in this system.

If, in fact, the radical SO$_2$•$^-$ was being formed in the reaction, it would require that the formyl radical, CHOO• also be formed. It is well known that the formyl radical is generally short lived and will quickly decay to CO$_2$ and H•.[64] The H• can go on to react with itself to form H$_2$ gas, or react with various other compounds in the system. While radicals are a relatively well studied field in terms of SO$_2$, since the radical anion is relatively stable and can be formed through both reduction in acid conditions and electrochemical methods, this particular reaction with a naked formate anion had yet to be reported.

Potteau *et al.*[45] found that the SO$_2$ radical will quickly form a dimer, which is the species that gives the characteristic blue colour observed in this reaction. This dimer can go on to form sulfur oxyanions such as dithionite. Such dianions could replace the

formate anion in the salt; they have no protons which explains why no new proton signals were observed in the ^{1}H NMR after the reaction. They are, however, strong reducing agents meaning they are easily oxidized by the atmosphere.
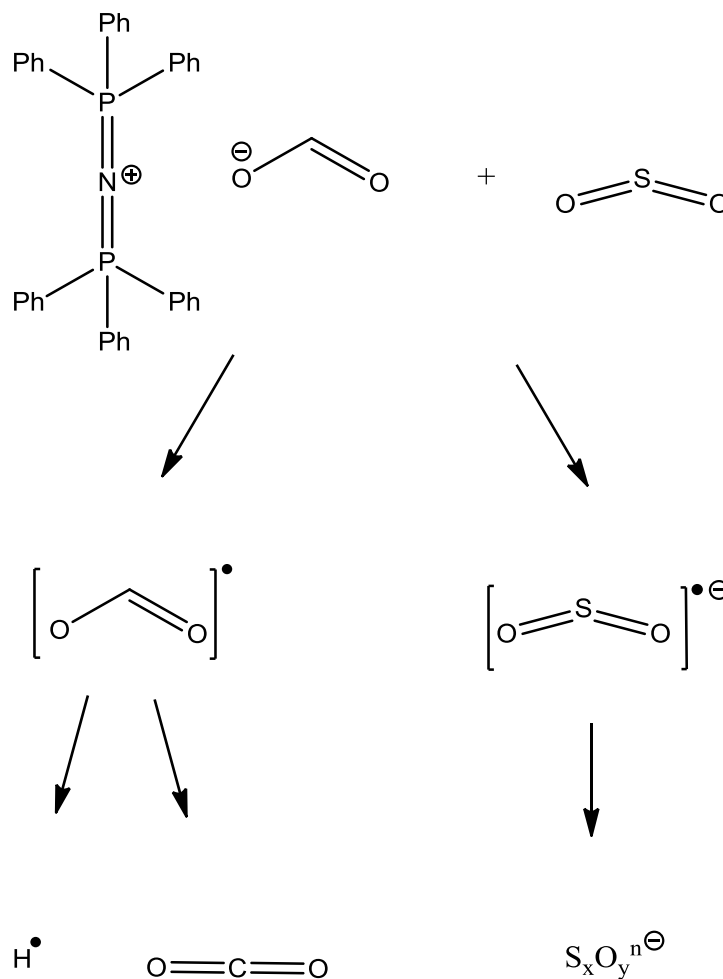
Scheme 9: Theorized reaction pathway for the radical reaction of SO$_2$ and [PNP]][CHOO].

The proposed reaction pathway gave us many different molecules that needed to be detected, including both the final products as well as the radical intermediates. As the final products should be the easiest to detect, that is where we started experimentally.

4.3 Detection of Gases Produced

To begin, the reaction was studied using *in situ* ReactIR in an attempt to detect CO_2 that much like the COS in the first reaction studied, would be partially soluble in MeCN. Solid [PNP][CHOO] was dissolved in acetonitrile and exposed to an SO_2 atmosphere while scans were taken every 30 seconds. The observed trends showed a steep drop in the peak at $1637 cm^{-1}$ which corresponds to the C=O stretching frequency of formate. This drop correlates very well with an observed spike in the height of the peak at $2355 cm^{-1}$ which is the asymmetric stretching frequency for CO_2.
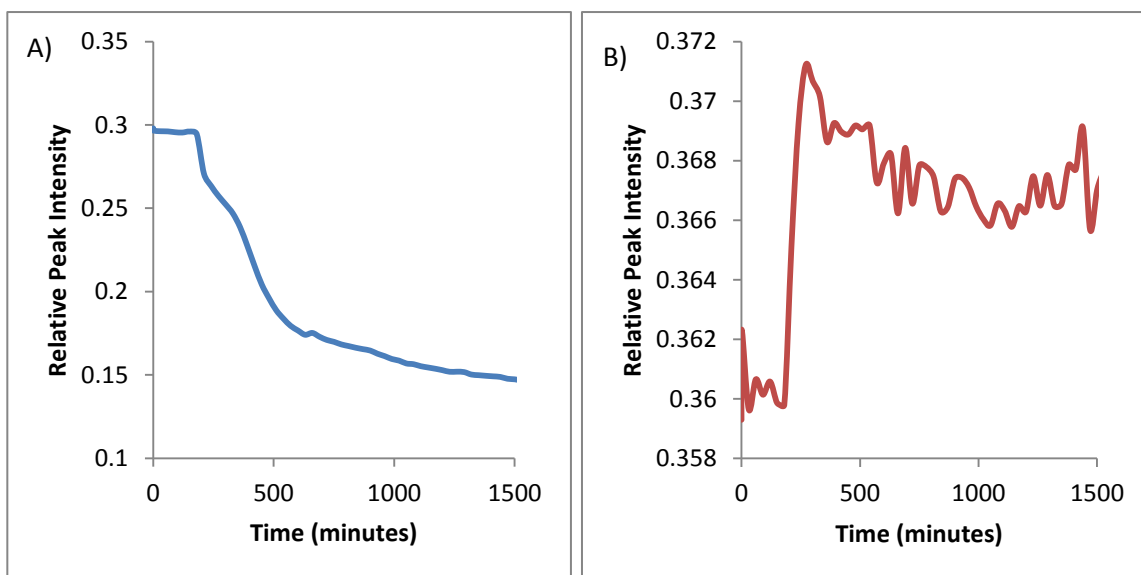
Figure 11: Peak trends for peaks at A) $1637 cm^{-1}$ and B) $2355 cm^{-1}$ in the infrared spectra recorded over time for the reaction of SO_2 and [PNP][CHOO].

There appears to be very little time difference between the decrease in the intensity of the formate peak and the appearance of the CO_2 peak, yet again implying that the reaction happens rapidly. The jagged peaks and relatively low intensity of the CO_2 peak can be explained by the fact that it is only partially soluble in MeCN, and therefore

upon formation would diffuse out of the solution, a process that would be aided by the constant stirring of the reaction.

To get a clearer picture of the evolution of CO_2, as well as to test if this reaction would happen with a solid/gas interaction, a small portion of [PNP][CHOO] was placed in an IR gas chamber with NaCl salt windows. The chamber was evacuated for the baseline reading then filled with SO_2 and the reaction tracked by taking a series of spectra over the following few hours. Upon the initial addition of SO_2 the salt almost immediately turned from white to a dark brown, started to melt from the heat being given off, and bubbled. However, there were no visual signs of reaction if sodium formate was used instead of the PNP salt. It is theorized that again (as with sodium acetate and CS_2) the smaller cation forms too stable a carboxylate salt and that a "naked" form of the anion is needed for the reaction to proceed easily.

With time, the spectra of the atmosphere above the solid/gas reaction showed the intensity of the SO_2 peaks dropping and a relative increase in the intensity of the CO_2 peaks. This, along with the ReactIR study of the solution, confirms that CO_2 is one of the final products. It also suggests that the SO_2 is being pulled out of the gas phase and into the solid phase by the reaction. If SO_2 was being converted into a different gaseous product, the peaks of that product would be observed in the IR of the atmosphere above the reaction, but no such peaks were observed.

Once CO_2 had been detected, there was very good supporting evidence that the formyl radical was also being produced in the reaction. As stated before, this is a very unstable species as the resulting degradation products, CO_2 and H_2 gas, are much lower in

energy. To detect the H_2 gas, [PNP][CHOO] was dissolved in MeCN in a Schlenk flask that was filled with a mixture of N_2 and SO_2 gas. Once the reaction had gone to completion (when the solution was a pale yellow), the atmosphere was sampled and run through a gas chromatograph. The chromatogram was standardized using pure H_2 gas samples, and a voltage detector was used to indicate the run times of the different gasses. While present in relatively small amounts compared to the other gases, H_2 gas was qualitatively detected in the atmosphere above the reaction. This gave evidence for the second formyl radical degradation product, as well as explaining why the peak in the ^1H NMR spectrum corresponding to the formyl proton disappeared after the reaction.

4.4 Observation of Sulfur/Oxygen Species

The last two compounds that needed to be detected were the $SO_2\bullet^-$ and the sulfur oxyanion product(s). It was already hypothesized that the sulfur oxyanion was becoming part of the solution or solid phase because the gas chamber IR showed a drop in SO_2 concentration without the production of a sulfur containing gas. More conclusive evidence of this came from a crystal isolated from the solution phase reaction. The crystal formed when the solvent was allowed to evaporate off while being exposed to the air. The salt that was formed was bis(triphenylphosphoranylidene)ammonium sulfate, ([PNP][SO_4H]).

It is likely that this salt is the product of the oxidation of the sulfur oxyanion produced by the initial reaction pathway. Since the initial reaction involved the oxidation of formate, it would be sensible for SO_2 to end up in a lower oxidation state after the radical reaction. Because these lower oxidation state polythionites are strong reducing

agents it means they could then easily be oxidized by the atmosphere to sulfate which was observed here.
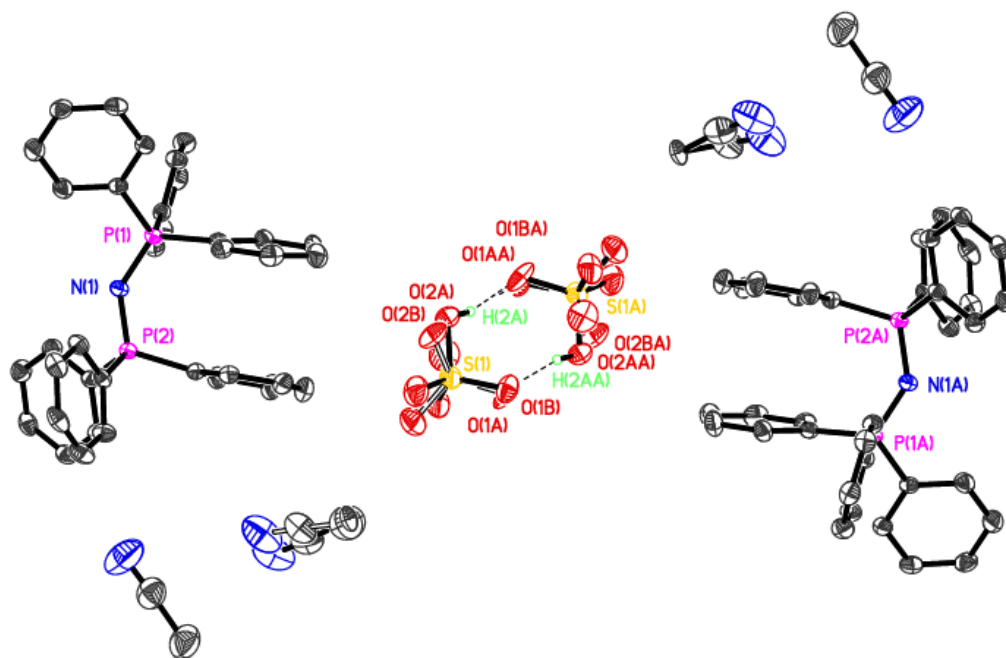
Figure 12: Crystal structure of [PNP][SO$_4$H] solvated with acetonitrile. Most of the hydrogen atoms have been removed for clarity. Thermal ellipsoids are drawn at the 50% probability level. The anions form a hydrogen bonded dimer in the solid state.

4.5 EPR Analysis

The final step of the characterization of this reaction was to detect the radical sulfur species. This was done by collecting a flat cell EPR of the solution phase reaction under an argon atmosphere. The solution reaction consisted of MeCN for the solvent, 18-crown-6, sodium formate and SO$_2$. It was found that, if 18-crown-6 was used to make

sodium formate soluble in MeCN, then the reaction would proceed just as it did with [PNP][CHOO]. The implication of this is that as long as the cation is bulky enough to leave the formate "naked" the exact cation does not make a difference. Due to its polarity MeCN is a relatively poor EPR solvent as solvents with higher dielectric constants can interfere with the sensitivity of the reading, but was chosen to keep this experiment consistent with the all previous trials. The use of the flat cell kept the MeCN volume to a minimum and allowed for a spectrum to be taken. The spectrum showed one peak with a calculated g value of 2.006 and a peak width at half height of approximately 2.9 G. These values correlate well with the values reported by Lough *et al.*[64] for the $SO_2\bullet^-$ radical anion. This test added a quantitative characterization to the qualitative observations and confirm that $SO_2\bullet^-$ is being formed in the reaction.
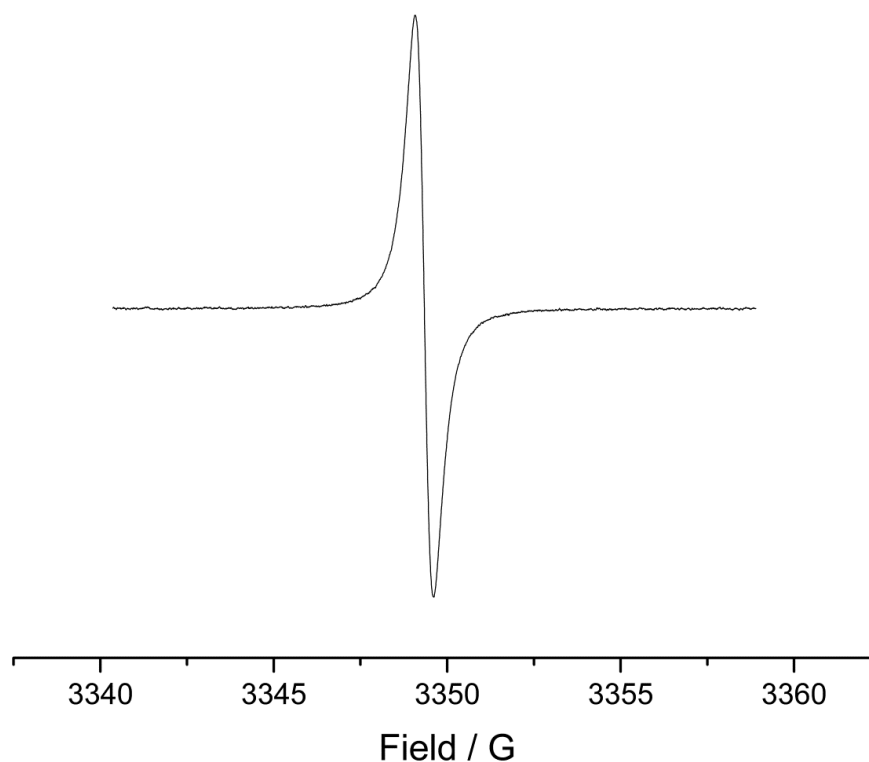
Figure 13: The EPR spectrum of PNP[HCOO] and SO$_2$ in MeCN.

A similar test was done by mixing together solid sodium formate, 18-crown-6 and sodium chloride before exposing the mixture to $SO_2$ gas. An EPR of the solid sample produced two weak peaks, one at 2.006 g that matched the solution phase reading attributed to the $SO_2\bullet^-$ radical anion. The other peak was observed at 2.000 g and while it has not been definitely identified, it is most likely a radical form of one of the sulfur oxyanions. The surprising thing about this measurement is that no reaction had been observed in the solid phase using sodium formate up until this point. While the reaction in the solid phase involving large, non-coordinating cations had gone quickly, there had been no observed reaction with the salts containing smaller cations. This reading shows that although the reaction goes much slower, it is not completely prohibited. This widens the scope of the reaction much more, particularly if it is being looked at in a prebiotic context. It is more likely that the formate salts formed in that period would have contained the more common, smaller cations such as sodium. If as previously thought this would have stopped the reaction from occurring completely, it would have been much more detrimental. However if the reaction can occur over a time frame measurable here, it is possible that over the thousands of year in which the prebiotic Earth developed the amount of polythionites produced by these reactions would have become relevant.

On the theme of the prebiotic relevance of these molecules, polythionites have been invoked on a number of occasions as energy sources for prebiotic systems.[65] As observed in the earlier reaction, with the isolation of [PNP][SO$_4$H] from the solution phase, these species are strong reducing agents and/or oxidizing agents. Their oxidation can release a significant amount of energy, and there are a number of microorganisms that

are capable of using them as energy sources. In the early prebiotic Earth, the atmosphere was still a reducing environment, as bacteria had not yet led to the oxidation of the planet. This would have stopped the polythionites from being oxidized before they could be used as energy sources.

The simultaneous production of H_2 gas in the system would also help to keep the environment from being too oxidizing. One of the biggest current debates about the prebiotic atmosphere is what percentage of H_2 was present. The formation of organic molecules is more favorable with higher concentrations of the gas present,[36] but most early models show H_2 escaping Earth's gravity early in the planet's formation and therefore making up only a very small portion of the atmosphere. Recent articles in Science have called these models into question.[67,68] While their suggestions have been debated, they calculated that the thermal escape would have been much slower than previously expected resulting in an H_2 concentration of as much as 0.1 bar. With the atmospheric concentration of H_2 being debated, this places more importance on high local concentrations of the gas. This is why the production of H_2, along with the other compounds produced in the reactions discussed in this thesis, could have played an important role on the prebiotic environment in which they occurred.

Chapter 5 – Summary and conclusions

In this project it has been shown that the interactions of small carboxylate anions and acid gases can have a wide range of possible outcomes. While the sought after adducts were not isolated, both an exchange mechanism and a radical reaction were observed. The exchange mechanism was shown to occur between the acetate anion and CS_2 through a bimolecular rate determining step, to produce thioacetate and COS both in solution and through solid/gas interactions. The radical reaction was observed between the formate anion and SO_2 and produced CO_2, H_2 and an $S_xO_y^{n-}$ species. It also occurred both in the solution phase and through solid/gas interactions. With both reactions producing molecules with potential prebiotic importance through very different mechanisms, the reactions of carboxylates with acid gases may, even yet, hold undiscovered chemistry.

Chapter 6 – Future Work

In the continuation of this project, the detection of the polythionite species (from the SO_2 - formate reaction) either by X-ray crystallography or by Raman spectroscopy will be one of the first steps carried out. This would allow better understanding of the reaction as a number of different polythionites have been reported to come from similar radical reactions. We also plan on adding a more extensive theoretical section to the work. For the reaction of acetate and CS_2 this would include an environment more appropriate to prebiotic Earth, while for the reaction of [PNP][HCOO] and SO_2 the goal would be to understand the reaction mechanism more thoroughly. Exploring these different environments will be part of the future experimental work as well; this exploration will require the introduction of other salts, expanding the variety of carboxylates that have been studied, and using aerosols or clays as different reaction media. In the reactions of CS_2 with some other carboxylates, similar colour changes were observed but time did not permit a full investigation to be carried out. Further experiments would be required to map out the general reactivity patterns, as well as the range of possible reactions. With the reaction of SO_2 the other carboxylates did not exhibit the same colour changes, implying that there may be something particular about formate, potentially the position of the hydrogen atom, that allows the radical reaction to occur. Exploring this hypothesis would require both computational and experimental research.

Chapter 7 – Experimental

7.1 General Procedures

All preparations were performed under an inert nitrogen atmosphere in either an mBraun glove box or by standard Schlenk line techniques, unless otherwise stated. Tetrabutylammonium acetate (97%), bis(triphenylphosphoranylidene)ammonium chloride (97%), sodium chloride, acetonitrile (99.8%, anhydrous), sodium formate (98%), tetrabutylammonium benzoate (98%), tetrabutylammonium bromide (99%), tetrabutylammonium fluoride (1.0M in THF), 1,4,7,10,13,16-hexaoxacyclooctadecane (99%) and tetrabutylammonium cyanide (94%) were purchased from Sigma Aldrich and used without any further purification. Carbon disulfide was purchased from Aldrich and was dried before use with magnesium sulfate. Sulphur dioxide and nitrogen (>99.998%) was provided by Praxair Inc. Reagent grade acetonitrile, dichloromethane and acetone were purchased from Caledon Laboratory Chemicals. Magnesium sulfate, and potassium bromide (infrared grade) were purchased from Fisher Scientific and were dried/stored in an oven prior to use. Benzne-D6 (D: 99.5%), Dichloromethane-D_2, Acetonitrile-D_3 (D: 99.6%) and DMSO-D_6 (D: 99.9%) were purchased from Cambridge Isotope Laboratories, Inc. and were opened/stored under nitrogen.

7.2 Spectroscopic Techniques

All infrared spectra were collected using a Bruker Vertex 70 Infrared Spectrometer as either liquid films on sodium chloride salt plates, KBr pellets or within a gas IR chamber with sodium chloride salt plates as its windows. Data processing was completed using the OPUS 6.0 software suite.

In situ infrared spectra were collected using a Mettler Toledo ReactIR 15. The data was initially analyzed using iC.IR 4.3 and plotted in Microsoft Excel 2010. Unless otherwise stated the reactions were performed under N_2 gas and with gentle stirring throughout the course of the reaction.

The NMR experiments were carried out on a Bruker Ultrashield 300 MHz NMR spectrometer with a 7.05 Tesla magnet. The samples were prepared by dissolving a small amount of the compound into an aliquot of the deuterated solvent under an inert atmosphere. ^1H and $^{13}C\{^1H\}$ spectra were referenced to residual solvent downfield of trimethylsilane. The data was processed using Bruker TOPSIN 1.3.

The melting points were measured using a Mel-Temp melting point apparatus (with a heating rate of *ca.* 5 °C min^{-1}) and are uncorrected. The samples were prepared by filling a capillary tube with a few milligrams of sample material and sealing the tube under an inert atmosphere if non air stable.

Gas chromatography for the detection of H_2 was done by Dr. Zhongmin Dong on a portable gas chromatograph made for his lab. The air compressor (4HP, 13 Gallon, 120 Maximum PSI and standard duty, made by Campbell Hausfeld) took gas from room atmosphere at room temperature. The compressed gas with pressure set at 7PSI flowed to a gas drying unit (drier $CaSO_4$ filled in a 29cm height and 7cm diameter bottle with two openings at top and bottom sides for connecting plastic tubes). The drying unit linked to a pressure gauge and then the injector. The injector was made by holding a rubber septum against a nut and a tee joint. The injector was connect to a GC column (2ft. long × 1/8in. × 0.85in.SS, coil shape, and packed with Porapak N 80/100, made by Alltech

Associates, Inc., serial No. 160 – 2982). The coil GC column was linked to the hydrogen sensor (QUBIT Systems Inc., order No. S121). Finally, the sensor joined to the interface and then to the computer. The computer loaded with Data Logger program (Vernier Software) was used to collect the data. For all experiments, the flow rate of the air pass through the GC column was 23 ml/min and the room temperature was recorded everyday for reference.

7.3 Solution State Screening for CS_2 Reactivity

0.5 millimoles each of tetrabutyl ammonium acetate, tetrabutyl ammonium benzoate, tetrabtuyl ammonium bromide, tetraethyl ammonium bromide, tetraphenyl phosphonium bromide, tetraphenyl phosphonium iodide, and tetrabutyl ammonium cyanide were placed in individual 20 mL scintillation vials. Enough acetonitrile was added to each to dissolve the solid (3-10 mL depending on solubility). Each vial was placed in an oven dried desiccator whose bottom was filled with DryRite. 1-2 drops of CS_2 was added to each vial and the dessecator was closed. Salts that showed signs of reaction (primarily colour change) were used in further testing.

7.4 Solution state screening for SO_2 reactivity

0.5 millimoles of ammonium acetate, sodium formate, tetrabutyl ammonium aceate, tetrabutyl ammonium benzoate, tetraphenyl phosphonium chloride, tetraphenyl phosphonium bromide, and bis(triphenylphosphoranyliden)ammonium formate were placed in individual 20 mL Scintillation vials and dissolved in enough acetonitrile to dissolve the solid (3-10 mL). These vials were placed in a vacuum desiccator while open, with 100 mL of toluene present as a counter solvent. The desiccator was evacuated and then filled with SO_2. The salts that displayed clear signs of reaction (primarily colour change) were used for further experiment.

7.5 Synthesis of important compounds
Tetrabutylammonium thioacetate

1 mmol of tetrabutyl ammonium aceate was dissolved in 3 mL of acetonitrile. 2 drops of

CS_2 were added, and the solution turned dark red. This solution was left in a dessicator

for the first 24 hours and then moved to a glove box were the solvent was allowed to

evaporate off. After the first 24 hours the solution also turned from red to orange. Long,

needle like crystals that were clear and colourless grew after 3 days and were removed

from the orange, gel like substance that remain in the vial. The crystals were identified as

tetrabutyl ammonium thioaceate by FT-IR, ^{1}H NMR, melting point and X-ray

crystallography.

^{1}H (300 MHz, CD_2Cl_2, ppm): 0.9728 (t, 12H, $^3J_{CH}$ = 7.35 Hz, -CH$_2$CH$_2$CH$_2$C$\underline{H_3}$) 1.35 (sep, 8H, $^3J_{CH}$ = 7.39 Hz, -CH$_2$CH$_2$C$\underline{H_2}$CH$_3$)1.6045 (m, 8H, -CH$_2$C$\underline{H_2}$CH$_2$CH$_3$) 2.15 (s, 2H, $^-$SOCC$\underline{H_3}$) 3.09 (t, 8H, $^3J_{CH}$ = 8.44, -C$\underline{H_2}$CH$_2$CH$_2$CH$_3$) IR (KBr, cm^{-1}): 2960(vs), 2875(s), 2734(vw), 1710(m), 1678(m), 1590(m), 1553(s), 1493(s), 1468(s), 1385(s) 1341(w), 1270(w), 1227(w), 1156(m), 1031(m), 1110(s), 1031(m), 947(s), 882(w), 804(m), 745(s), 671(m), 617(w), 518(s,b) HRMS calcd. [m/z]: 339.2028; found [m/z]: 339.2074.

Solid state synthesis of tetrabutylammonium thioacetate.

1 mmol of tetrabutyl ammonium acetate was placed in a 100 mL Schlenk flask and sealed

under vacuum with a rubber septum. Approximately 5 mL of carbon disulfide was placed

in a separate 100 mL Schlenk flask that was evacuated and then refilled with N_2. A needle

was used to remove 5 mL of the gas in the carbon disulfide Schlenk flask and inject this

into the tetrabutyl ammonium acetate flask. The solid was allowed to react until the full

colour change of the solution phase reaction was observed (white to red to orange) before

the flask was evacuated again.

^{1}H (300 MHz, DMSO, ppm): 0.93 (t, 12H, $^3J_{CH}$ = 7.35 Hz, -CH$_2$CH$_2$CH$_2$C$\underline{H}_3$), 1.30 (sep, 8H, $^3J_{CH}$ = 7.39 Hz, -CH$_2$CH$_2$C$\underline{H}_2$CH$_3$) 1.56 (m, 8H, -CH$_2$C$\underline{H}_2$CH$_2$CH$_3$) 1.76 (s, 3H, $^-$SOCC$\underline{H}_3$) 3.16 (t, 8H, $^3J_{CH}$ = 8.44, -C$\underline{H}_2$CH$_2$CH$_2$CH$_3$)   IR (Gas chamber, NaCl windows, cm^{-1}): 2960 (vw), 2360 (w), 2333 (w), 2319 (w), 2192 (m), 2179 (m), 2071 (m), 2052 (w), 1576 (w), 1545 (s, b), 1261 (w), 1017 (w), 885 (w), 799 (w), 670 (w), 621 (w), 464 (s), 448 (s), 419 (s), 409 (s)

Bis(triphenylphosphoranylidene)ammonium formate

In a 250mL Erlenmeyer flask 2.5 g of bis(triphenylphosphoranyliden)ammonium chloride (PNPCl) was dissolved in 100mL of boiling water. In a 1 L Erlenmeyer flask 24.8 g of sodium formate (NaHCOO) was dissolved in 300mL of boiling water. Both solutions were stirred throughout the reaction using a magnetic stir plate. The PNPCl solution was added to the NaCHOO solution in small portions, allowing the solution to clear in between each addition. When needed extra water was added to the solution to clear it, leading to a total solution volume of 800mL at the end. At this point a small amount of white precipitate could be observed. The flask was removed from heat and cooled to room temperature before being moved to a fridge and stored at 5°C for two hours before the solid was collected by vacuum filtration. The product was rinsed with three 20mL portions of diethylether to dry. Melting point, ^{1}H NMR and FT-IR were collected on the solid.

mp = 84-87°C ^{1}H (300 MHz, CD$_3$CN, ppm): 7.56 (m, 30H, Ar), 8.56 (s, 1H, $^-$O$_2$C$\underline{H}$) IR (KBr, cm^{-1}): 3658(w), 3052(m), 3022(m), 2958(w), 2809(w), 1610(s), 1586(s), 1482(m), 1436(s), 1370(w), 1345(m), 1310(m,b), 1274(s,b), 1182(m), 1160(w), 1114(s), 1023(w) 997(m), 798(w), 763(m), 749(m), 726(s), 694(s), 616(w), 536(s), 499(s), 457(w), 446(w)

Solution reaction of bis(triphenylphosphoranylidene)ammonium formate with SO$_2$

0.9 g of [PNPHCOO] were dissolved in 15 mL of acetonitrile in a 100 mL Schlenk flask.
The flask was then evacuated and filled with SO$_2$. The solution, which immediately
turned a dark royal blue, was allowed to stir overnight before being evacuated again and
opened to the atmosphere. Crystals of PNPHSO$_4$ formed in the solution as the solvent
evaporated and were collected for FT-IR, ^{1}H NMR and X-ray crystallography.

^{1}H (300 MHz, CD$_3$CN, ppm): 7.53 (m, 30H, Ar) 8.65 (s, 1H, SO$_4$H) IR (NaCl plates, cm$^-$^{1}): 3622(w,b), 3541(w), 3202(w), 3003(m), 2944(m), 2293(m), 2253(vs), 1632(w,b), 1441(s,b), 1376(s), 1334(w), 1170(w), 1039(m), 919(m), 750(w), 726(w), 696(w)

Solid state reaction of of PNP(CHOO) with SO$_2$

Approximately 0.1 g of [PNPHCOO] were placed in a 50 mL Schlenk flask which was
evacuated and then filled with SO$_2$. The solid immediately turned dark brown, bubbled,
and gave of heat. FT-IR and ^{1}H NMR were done on the solid. FT-IR spectra of the
atmosphere above the reaction were taken as the reaction progressed which was repeated
in an IR gas chamber.

^{1}H (300 MHz, CD$_3$CN, ppm): 7.56 (m, 24H, aryl) 7.71 (m, 6H, aryl) IR (KBr, cm^{-1}):
3495(w,b), 3057(m), 3022(m), 1657(w,b), 1587(m), 1482(s), 1439(s), 1251(s,b) 1181(s)
1114(s), 1058(s), 1012(s), 997(s) 832(m), 800(m), 750(s), 724(s), 693(s), 642(m),
593(m), 552(s), 532(s),497(s), 443(w) IR (Gas Chamber, NaCl window, cm^{-1}): 2963 (w),
1529 (w), 1373 (vs), 1357 (vs), 1166 (m), 1137 (m) 799 (w), 623 (w) 454 (s), 432 (s)

7.6 EPR analysis of the reaction of Na(CHOO) with SO$_2$

The experimental in 7. for the solution phase reaction of PNP(CHOO) with SO$_2$ was followed to prepare the solution however the PNP(CHOO) was replaced with sodium formate and an excess of 18-crown-6. A septum was placed on either end of a flat cell and a needle inserted to allow argon gas to pass through the cell for 10 minutes. A needle was then used to insert a small portion of the liquid sample. The sample was allowed to run to the bottom before the cell was sealed, after which the spectrum was collected. The spectrum had a single peak at 2.006g and a half height of 2.9G.

The solid state spectrum was collected by mixing together solid sodium chloride, 18-crown-6 and sodium formate. This mixture was exposed to an atmosphere of SO$_2$ before evacuating the flask and transferring the solid to an EPR tube under an inert atmosphere. Multiple scans were performed to cancel out the noise and produce a spectrum containing two weak signals at 2.006g and 2.000g. All EPR experiments were performed on a Magnettech GmbH MiniScope 200 X-band EPR spectrometer by Juha P. Hurmalainen at the University of Jyväskylä.

7.7 Theoretical calculation details

All computations were performed using the Spartan '14 software package,[61] unless otherwise stated. All *ab initio* computations performed with Spartan were first drawn using the graphical interface, followed by computing the equilibrium conformation *via* semi-empirical PM3[62] methods. The lowest energy conformations were then used as the initial geometries for DFT calculations of the equilibrium geometry at the B3LYP[63,64] level of theory, using the 6-31G* basis set. The energy output was in units of hartrees and

was converted to units of kJ mol^{-1} with a conversion factor of; 1 Ha = 2625.5 kJ mol^{-1}.

The overall bonding energy was taken as the difference between the total free energy of the adduct minus the total free energies of the gas and the acetate anion calculated at the same level of theory.

7.8 Infrared Kinetics Study

All trials were set up using 15 mL of anhydrous MeCN and the necessary amount of TBAA and CS_2. The rate was determined by allowing the reaction to go until there was no longer any change in the peak height of the peak of TBAA at 1592cm^{-1}. This was taken to be 100% of the TBAA converted as CS_2 was in excess for each reaction. The percentage of the TBAA converted was then calculated between the initial concentration and final endpoint, which was then converted into the number of moles after 3 minutes of the reaction. Details on the ReactIR can be found in 8.2.

7.9 X-Ray Crystallography Refinement

The crystal chosen for each determination was attached to the tip of a 400 μm MicroLoop with paratone-N oil. Measurements were made on a Bruker APEXII CCD equipped diffractometer (30 mA, 50 kV) using monochromated Mo Kα radiation (λ = 0.71073 Å) at 125 K.[69] The initial orientation and unit cell were indexed using a least-squares analysis of a random set of reflections collected from three series of 0.5° ω-scans, 15 seconds per frame and 12 frames per series, that were well distributed in reciprocal space. For data collection, four ω-scan frame series were collected with 0.5° wide scans, 30 second frames and 366 frames per series at varying φ angles (φ = 0°, 90°, 180°, 270°). The crystal to detector distance was set to 6 cm and a complete sphere of data was collected. Cell refinement and data reduction were performed with the Bruker SAINT[70]

software, which corrects for beam inhomogeneity, possible crystal decay, Lorentz and polarisation effects. A multi-scan absorption correction was applied (SADABS[71]). The structures were solved using SHELXT-2014[72] and were refined using a full-matrix least-squares method on F^2 with SHELXL-2014[72]. All refinements were unremarkable. The non-hydrogen atoms were refined anisotropically. Hydrogen atoms bonded to carbon were included at geometrically idealized positions and were not refined. The isotropic thermal parameters of the hydrogen atoms were fixed at $1.2U_{eq}$ of the parent carbon atom or $1.5U_{eq}$ for methyl hydrogens. In certain cases a disordered model was found to be best for methyl groups showing rotational motion. Such groups were best defined using an idealized disordered model with two sets of equally occupied positions, rotated from each other by 60 degrees. Each hydrogen in a disordered group was thus given an occupancy of 0.5. Crystal structure images were drawn using Mercury 3.5.1[73]

Both the SO_4H^- anion and one of the acetonitrile solvent molecules in the crystal structure of $[PNP][SO_4H] \cdot 2CH_3CN$ were found to be disordered. The oxygen atoms of the anion were split over two sets of positions, with the occupancies of each group refined to 92% and 8%, respectively. Pairs of anions form hydrogen bonded dimers in the structure. In the predominant group, the hydrogen atom was located on O2A, while in the minor group it was located on O3B. The S−O bond lengths and the O···O distances within each anion were restrained to be equal during the refinement. In addition, all of the oxygen atoms in the anion were restrained to have similar thermal parameters. The atoms of the disordered acetonitrile solvent molecule were also split over two positions. The occupancies of the two parts refined to 36% and 64%, respectively. All of the bond lengths in the molecule were restrained to be equal between the two parts. The thermal

parameters of equivalent atoms in the two parts were also restrained to be similar during the refinement.

References

1. Gandhi, T.; Jagirdar, B. R. *Inorg. Chem*. **2005**. 44, 1118.
2. Anderson, J. S.; Iluc, V. M.; Hillhouse, G. L. *Inorg. Chem*. **2010**. 49, 10203.
3. Vol'pin, M. E.; Koloukov, I. S. *Pure Appl. Chem*. **1973**. 33, 567.
4. Yu, T.; Yamada, T.; Weiss, R. G. *Chem. Mater*. **2010**. 22 (19), 5492.
5. Chaturvedi, D.; Ray, S. *Tetrahedron Lett*. **2006.** 44, 1307\.
6. George, M.; Weiss, R. G. *Langmuir*. **2003**. 19, 1017.
7. Decaprio, A. P.; Spink, D. C.; Chen, X.; Fowke, J. H.; Zhu, M. Bank, S. *Chem. Res. Toxicol*. **1992**. 5, 496.
8. Brown, W.; Hoel, A. B. *J. Am. Chem. Soc*. **1922**. 44, 2315.
9. Lieber, E.; Pilli, C. N.; Ramachandran, J.' Hites, R. D. *J. Org. Chem*. **1957.** 22, 1750.
10. Perman, C. A.; Gleason, W. B. *Acta. Cryst*. **1991.** C47, 1018.
11. Hoffmann, A.W. *Bericht*. **1880**, 13, 1732.
12. Ghiassi, K. B.; Walters, D. T.; Aristov, M. M.; Loewen, N. D.; Berben, L. A.; Rivera, M.; Olmstead, M. M.; Balch, A. L. *Inorg. Chem.* **2015.** 54, 4565.
13. Chaturvedi, D.; Ray, S. *Tetrahedron Lett.* **2005.** 47 (8), 1307.
14. Anderson, J. S.; Iluc, V. M.; Hillhouse, G. L. *Inorg. Chem.* **2010.** 49, 10203.
15. Koeplinger, K. A. Report. **1987.** 205.
16. Bahr, G.; Schleitzer, G. *Chem. Ber.* **1955**, 88, 1771.
17. Zhang, X.; Gross, U.; Seppelt, K., *Angew. Chem., Int. Ed. Engl.* **1995**. 34, 1858
18. Murphy, L. J.; Robertson, K. N.; Harroun, S. G.; Brosseau, C. L.; Werner-Zwanziger, U.; Moilanen, J.; Tuononen H. M.; Clyburne, J. A. C. *Science*. **2014**. 344, 75.
19. Murphy, L. J.; Robertson, K. N.; Kemp, R. A.; Tuononen, H. M.; Clyburne, J. A. C. *Chem Commun.* **2015.** 51, 3942.
20. Heldebrant, D. J.; Yonker, C. R.; Jessop, P. G.; Phan. L. *Chem. Eur. J.* **2009.** 15 (31), 7619.
21. Cabaço, M. I.; Besnard, M.; Chávez, F. V.; Pinaud, N.; Sebastião, P. J.; Coutinho, J. A. P.; Danten, Y. *J. Chem. Phys*. **2014.** 140, 244307.
22. Dinse, K. P.; Mobius, K. *Teil A*. **1968**. 23, 695.
23. Lork, E.; Mews, R.; Viets, D.; Watson, P. G.; Borrmann, T.; Vij, A.; Boatz, J. A.; Christe, K. O. *Inorg. Chem.* **2011**. *40*, 1303.
24. Christe, K.; Boatz, J. A.; Gerken, M.; Haiges, R.; Schneider, S.; Schroer, T.; Tham, F. S.; Vij, A.; Vij, V.; Wagner, R. I.; Wilson, W. W. *Inorg. Chem.* **2002**. 41, 4275.
25. Kuhn, N.; Bohnen, H.; Bläser, D.; Boese, R.; Maulitz, A.H. *J. Chem. Soc., Chem. Commun.* **1994**. 2283.
26. Eller; P.G.; Kubas, G.J. *Inorg. Chem.* **1978**. *17*, 894.
27. Seel, F.; Herstellung von Salzen der Fluorsulfinsaeure. DE1000354 (B). January 10 1957.
28. Seel, F.; Ballreich, K.; Schmutzler, R. *Chemische Berichte.* **1962**. 95, 199.
29. Lork, E.; Mews, R.; Viets, D.; Watson, P.G.; Borrmann, T.; Vij, A.; Boatz, J. A.; Christe, K. O. *Inorg. Chem.* **2011**. *40*, 1303.
30. Helz, G.; Kosak-Channing, L. *Environ. Sci. Technol.* **1984**. 18 (2), 48A.

31. *Wastewater Technology Fact Sheet: Dechlorination.* EPA 832-F-00-022, United States Environmental Protection Agency, September 2000.
32. Ough, C.S.; Crowell, E.A. *J. Food Sci.* **1987.** 52 (2), 386.
33. Chichester, C.O. Sulfites in foods: uses, analytical methods, residues, fate, exposure assessment, metabolism, toxicity, and hypersensitivity. In *Advances in Food Science.* Academic Press Inc. 30, 2-64.
34. Clark, P.D. Sulfur and Hydrogen Sulfide Recovery. Alza, S., *Eds. Kirk-Othmer Encyclopedia of Chemical Technology*. **2007**. 23, 597.
35. Khanmamedox, T. K.; Welland, R. H. *Sulphur*. **2013.** 345, 62.
36. Liu, W.; Sarofim, A. F.; Flytzani-Stephanopoulos. *M. Appl. Catl. B.* **1994**. 4, 167.
37. Carter, H. A. *J. Chem. Educ.* **1996**. 73 (11), 1068
38. Shang, J.; Zhang, Y.; Zhou, F; Lv, F.; Han, F.; Lu, J.; Meng, X.; Chu, P. K.; Ye, Z.; Xing, J. *J. Hazard. Mater*. **2011**, 169, 65.
39. Lough, S. M.; McDonald, J. W. *Inorg. Chem.* **1987**, 26 (13), 2024.
40. Neta, P.; Huie, R.E.; Ross, A.B. J. *Phys. Chem. Ref. Data.* **1988.** 17, 1027.
41. Hayon, E.; Treinin, A.; Wilf, J. *J. Am. Chem. Soc.* **1972**. 94 (1), 47.
42. Streeter, I.; Wain, A. J.; Davis, J.; Compton, R. G. *J. Phys. Chem. B.* **2005.** 109 (39), 18500.
43. Li, R.; Alconcel, L. N. S.; Continetti, R. E. *Chem. Phys. Lett.* **2001.** 336, (1-2), 81.
44. Gardner, C. L.; Fouchard , D. T.; Fawcett, W. R. J. *Electrochem. Soc*. **1981**. 128, 2337.
45. Potteau, E.; Levillain, E.; Lelieur, J. P. *New J. Chem.*, **1999**, 23, 1117.
46. Shao, Y.; Molnar, L. F.; Jung, Y.; Kussmann, J.; Ochsenfeld, C.; Brown, S. T.; Gilbert, A. T. B.; Slipchenko, L. V.; Levchenko, S. V.; O'Neill, D. P.; DiStasio, R. A.,Jr; Lochan, R. C.; Wang, T.; Beran, G. J. O.; Besley, N. A.; Herbert, J. M.; Yeh Lin, C.; Van Voorhis, T.; Hung Chien, S.; Sodt, A.; Steele, R. P.; Rassolov, V. A.; Maslen, P. E.; Korambath, P. P.; Adamson, R. D.; Austin, B.; Baker, J.; Byrd, E. F. C.; Dachsel, H.; Doerksen, R. J.; Dreuw, A.; Dunietz, B. D.; Dutoi, A. D.; Furlani, T. R.; Gwaltney, S. R.; Heyden, A.; Hirata, S.; Hsu, C.; Kedziora, G.; Khalliulin, R. Z.; Klunzinger, P.; Lee, A. M.; Lee, M. S.; Liang, W.; Lotan, I.; Nair, N.; Peters, B.; Proynov, E. I.; Pieniazek, P. A.; Min Rhee, Y.; Ritchie, J.; Rosta, E.; David Sherrill, C.; Simmonett, A. C.; Subotnik, J. E.; Lee Woodcock, H.,III; Zhang, W.; Bell, A. T.; Chakraborty, A. K.; Chipman, D. M.; Keil, F. J.; Warshel, A.; Hehre, W. J.; Schaefer, H. F.,III; Kong, J.; Krylov, A. I.; Gill, P. M. W.; Head-Gordon, M. *Phys. Chem. Chem. Phys.* **2006**, *8*, 3172.
47. Lee, C.; Yang, W.; Parr, R. G. *Phys. Rev. B*. **1998**. *37*, 785.
48. Becke, A. D. *J. Chem. Phys.* **1993**. *98*, 5648.
49. Mendelsohn, R.; Monse, E. U. *J. Chem. Ed.* **1981.** 58, 582.
50. Ito, K.; Bernstein, H. J. *Can. J. Chem.* **1956.** 36, 170.
51. Nyquist, R. A.; Putzig, C. L.; Leugers, M. A. *Handbook of Infrared and Raman Spectra of Inorganic Compounds and Organic Salts.* Gulf Professional Publishing ,**1986**.
52. Ling, L.; Zhang, R.; Han, P.; Wang, B. *J. Mol. Model.* **2012**. 18, 1625.

53. Halmer, M. M.; Schmincke, H. -U.; Graf, H. -F. J. *Volcanol. Geotherm. Res.* **2002.** 115 (3-4), 511.
54. Chin. M.; Davis, D. D. *Global Biogeochem. Cy.* **1993.** 7 (2), 321.
55. Bretti, C.; De Steffano, C.; Foti, C.; Giuffè, O.; Sammartano, S. *J. Solutions Chem.* **2009.** 38, 1225.
56. Selsiss, F. *Astrophys. Space Sci. Libr.* **2004.** 305, 267.
57. Parker, E. T.; Cleaves, H. J.; Callahan, M. P.; Dworkin, J. P.; Glavin, D. P.; Lazcano, A.; Bada, J. L. *Orig. Life. Evol. Biosph.* **2011.** 41 (6), 569.
58. Kricheldorf, H. R. *Angew. Chem. Int. Ed.* **2006**, 45, 5752.
59. Leman, L.; Orgel, L.; Ghadiri, M. R. *Science.* **2004.** 306 (5694), 283.
60. Robineau, M.; Zins, D.; Brianso-Perucaud, M. C. *Rev. Chim. Miner.* **1975.** 12 (5), 440.
61. Silber, P.; Robineau, M.; Zins, D.; Brianso-Perucaud, M. C. *C. R. Acad. Sci.* **1975.** 280 (25), 1517.
62. Bueno, W.A. *An. Acad. Bras. Ciênc.* **1979.** 51 (1) 83.
63. Green, J. A., II; Young, D. C. *Preparation of oligomeric thiocarbonates as pesticides.* WO 9109526 A2. July 11, **1991**.
64. Hochanadel, C. J.; Sworski, T. J.; Ogren, P. J. *J. Phys. Chem.* **1980**. 84 (3), 231.
65. Lough, S.M.; McDonald, J.W. *Am. Chem. Soc.* **1987.** 26 (13), 2024-2027.
66. Kurth, J. M.; Dahl, C.; Butt, J .N. *J. Am. Chem. Soc.* **2015**, 137 (41), 13232.
67. Chyba, C. F. *Science.* **2005**. 308, 962.
68. Tian, F.; Toon, O.B.; Pavlov, A .A.; De Sterck, H. *Science*. **2005**, 308, 1014.
69. APEX II (Bruker, 2008) Bruker AXS Inc., Madison, Wisconsin, USA.
70. SAINT (Bruker, 2008) Bruker AXS Inc., Madison, Wisconsin, USA.
71. SADABS (Bruker, 2009) Bruker AXS Inc., Madison, Wisconsin, USA.
72. Sheldrick, G.M. (2008) *Acta Cryst*., A64, 112-122; Sheldrick, G.M. (2015) *Acta Cryst*., A71, 3-8; Sheldrick, G.M. (2015) *Acta Cryst*., C71, 3-8.
73. Macrae, C. F., Bruno, I. J., Chisholm, J. A., Edgington, P. R., McCabe, P., Pidcock, E., Rodriguez-Monge, L., Taylor, R., van de Streek, J. & Wood, P. A. *J. Appl. Crystallogr.* **2008**. 41, 466-470.